Microfluidic single-cell technology in immunology and antibody screening

CrossMark

Yu Fen Samantha Seah [1], Hongxing Hu [1], Christoph A. Merten[*]

European Molecular Biology Laboratory (EMBL), Genome Biology Unit, Meyerhofstrasse 1, Heidelberg, Germany

ABSTRACT

Single-cell technology has a major impact on the field of immunology. It enables the kinetics and logic of immune signaling and immune cell migration to be elucidated, facilitates antibody screening and allows massively parallelized analysis of B- and T-cell repertoires. Impressive progress has been made over the last decade, strongly boosted by microfluidic approaches. In this review, we summarize the most powerful microfluidic systems based on continuous flow, nanowells, valves and droplets and we analyze their benefits for phenotypic characterization, drug discovery and next generation sequencing experiments. We describe current limitations and provide an outlook on important future applications.

© 2017 The Authors. Published by Elsevier Ltd. This is an open access article under the CC BY-NC-ND license (http://creativecommons.org/licenses/by-nc-nd/4.0/).

1. Introduction

Immunology is a major field in modern medicine: antibodies have become the fastest growing class of all prescription drugs (Ecker et al., 2015) and detailed knowledge of immune signaling, immune cell migration and immune repertoires helps to develop therapeutics to fight diseases ranging from allergies and infections to cancer and aging (Liu and Mardis, 2017; Michel et al., 2016; Chen and Flies, 2013; Brownlie and Zamoyska, 2013; Tscharke et al., 2015). However, many molecular details in immunology can only be addressed on the single-cell level. For example, large variation has been observed for signaling events such as the stimulation of T-cells, requiring sophisticated experimental setups to derive mechanistic insights. Furthermore, the recombination events in B- and T-cells create extremely heterogeneous populations, and functional properties can hence only be analyzed at the single-cell level. In this review, we summarize the latest approaches to tackle these issues (Fig. 1) and to understand their functional implications. We look particularly at microfluidic platforms pushing current limits and enabling entirely new approaches.

Microfluidic chips consist of small channels, typically with a sub-millimeter diameter (Vyawahare et al., 2010). They are manufactured in clean rooms using specialized lithography equipment (Eicher and Merten, 2011) (Fig. 2A), but non-specialist labs can get access to the technology through academic facilities or commercial providers. For example, microfluidic chips can be obtained from Dolomite, Microfluidic Chip Shop, Microliquid, Simtech, or Flowjem for a few hundred (preexisting designs) to a few thousand (custom-made chips) dollars. However, further equipment, such as pumps and microscopes, is required to run experiments. Many companies (such as Fluidigm, 10X Genomics, Cellular Research, BioRad/Raindance Technologies and Sphere Fluidics) also offer complete instruments for particular applications, where the platforms cost up to several hundred thousand dollars with an additional reagent cost of a few hundred dollars per sample.

In general, the microfluidic platforms discussed here can be grouped into four different categories (Fig. 2B–E): i) continuous flow systems, ii) nanowells, iii) valve-based microfluidics and iv) droplet-based microfluidics. In a continuous flow system (Fig. 2B), reagents are injected into channels or networks thereof without any further possibility for compartmentalization. In other words, all reagents get in contact with each other and typically flow through the entire chip. Such systems can be exploited for generating stable gradients to perform chemotactic assays. However, different samples cannot be processed in parallel. The technically simplest implementation of parallelization is the use of miniaturized wells ("nanowells"; up to several hundred thousand per chip, Fig. 2C) capturing individual cells or reagents immobilized on beads (Upert et al., 2010). Another way of generating separate samples on the same microfluidic chip is to use valves to close off particular sections of the channel network, enabling independent reactions to be carried out (Fig. 2D). This way, a few thousand reaction chambers can be generated. Furthermore, the valves can be opened and

---

* Corresponding author.
  E-mail address: merten@embl.de (C.A. Merten).
[1] These authors contributed equally.
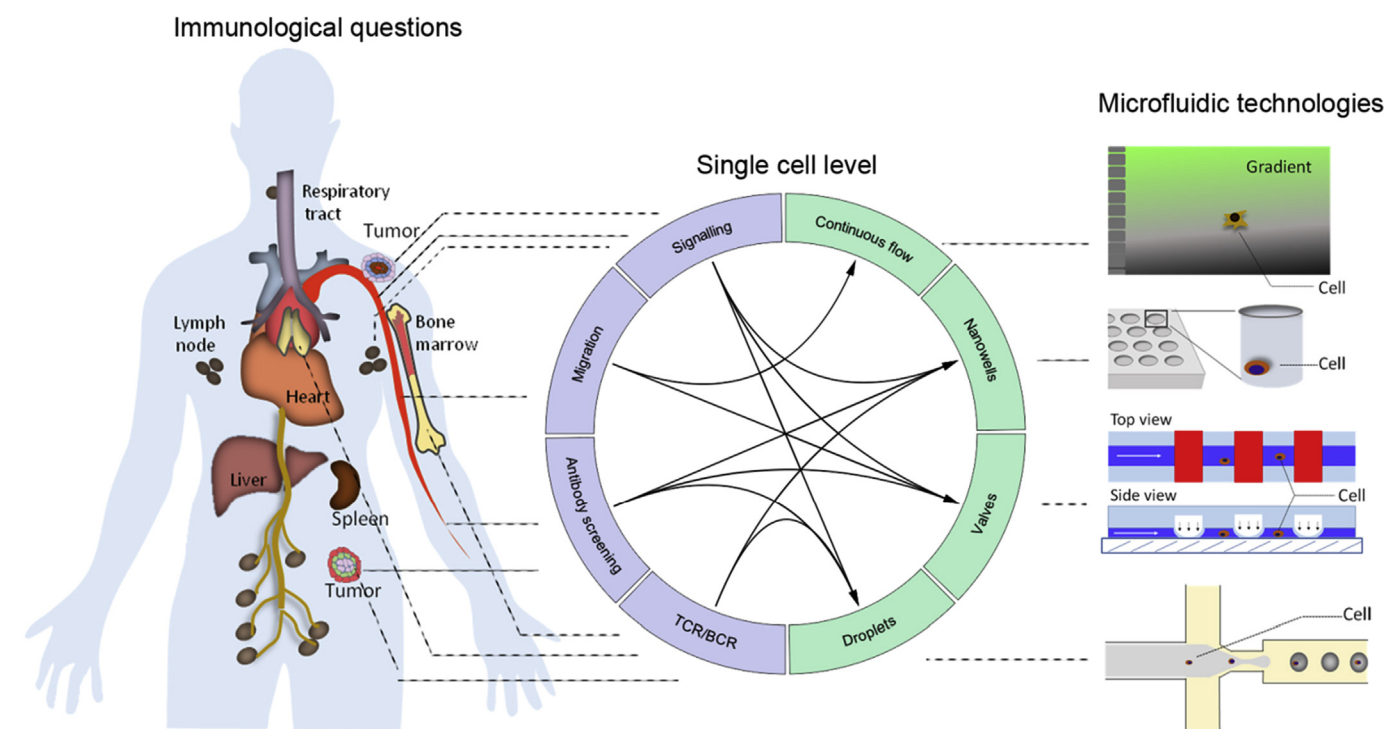
Fig. 1. Immunological questions which can be addressed by microfluidic technologies at a single-cell level. These include signaling, migration, antibody screening and the study of T- and B-cell receptor repertoires (purple), and these can be studied with continuous flow, nanowells, valves and droplets (green). (For interpretation of the references to colour in this figure legend, the reader is referred to the web version of this article.)

closed on demand, thus allowing complex manipulation steps (e.g. changing the media, adding further reagents, etc.). Reactions can also be compartmentalized in droplets surrounded by oil or air: Co-injecting an aqueous phase containing all reagents (optionally including cells) and a fluorinated immiscible oil phase into a microfluidic droplet maker results in the generation of an emulsion with very uniform droplet size (typically between 10 and 200 μm in diameter; Fig. 2E). This way, thousands of individual compartments can be generated per second, stabilized by surfactants (reducing the surface tension) to avoid droplet fusion upon contact. In consequence, millions of droplets can be stored off-chip in test tubes and analyzed or manipulated at later time points. Cells and reagents can also be recovered, by breaking the droplets upon addition of chemicals such as perfluoro-octanol, repeated freeze/thaw cycles or the application of electric fields. With all the methods mentioned, the aqueous and oil phases can be separated and the contents easily accessed and applied to downstream procedures (e.g. sequencing, cultivation of cells). Droplets can also be sorted according to fluorescence signals, enabling phenotypic screening, including complex assays with soluble substrates and/or secreted molecules (discussed in more detail in the section about antibody screening below). Instead of oil, one can also use air as the separation media for droplets, an approach which has been particularly exploited in digital microfluidics (Choi et al., 2012). Here, droplets are manipulated on top of an electrode array. Powering the electrodes changes the contact angle of the droplets on the surface of the chip, and using many neighboring electrodes even allows more complex operations (e.g. droplet movement, splitting and fusion). However, while this technology offers a superb level of control, typically no more than 100 samples can be processed. However, assays requiring proliferation are difficult to carry out in droplet- and digital microfluidics, given the limited nutrients present within each droplet. In general, long-term assays are problematic in non-

perfusion microfluidic systems, as the inability to exchange media limits the viability of cells over long periods of time. In addition, most automated microfluidic assays still require significant starting material, usually more than twenty thousand cells.

Readers interested in more details about microfluidic technology are referred to other reviews (Hummer et al., 2016; Shembekar et al., 2016; Xi et al., 2017). Here, we want to focus more on the applications in immunology, grouped into four different chapters (Fig. 2):

i) **Immune signaling.** Analyzing immune cells in microfluidic systems enables high spatiotemporal control. Reagents (e.g. for stimulation) can be precisely delivered to individual cells and cells can be paired on demand (e.g. an antigen-presenting cell and a T-cell). Simultaneous collection of quantitative, multiparameter data (e.g. imaging, transcriptome analysis, detection of secreted factors) reveals molecular mechanisms in great detail.

ii) **Immune cell migration.** Microfluidics allows the generation of stable gradients that can be controlled in time and space. Hence, complex chemotactic behaviors and other factors involved in migration can be analyzed.

iii) **Phenotypic screens for antibodies with desired properties.** Based on small assay volumes in droplet- and valve-based systems, detectable concentrations of secreted molecules (such as IgGs) can be obtained from single cells.

iv) **Screening the B- and T-cell repertoire.** Microfluidic technology allows the compartmentalization of individual cells and the amplification of specific genes or even the entire transcriptome in a highly parallelized fashion (e.g. for the sequencing of paired immunoglobulin genes).
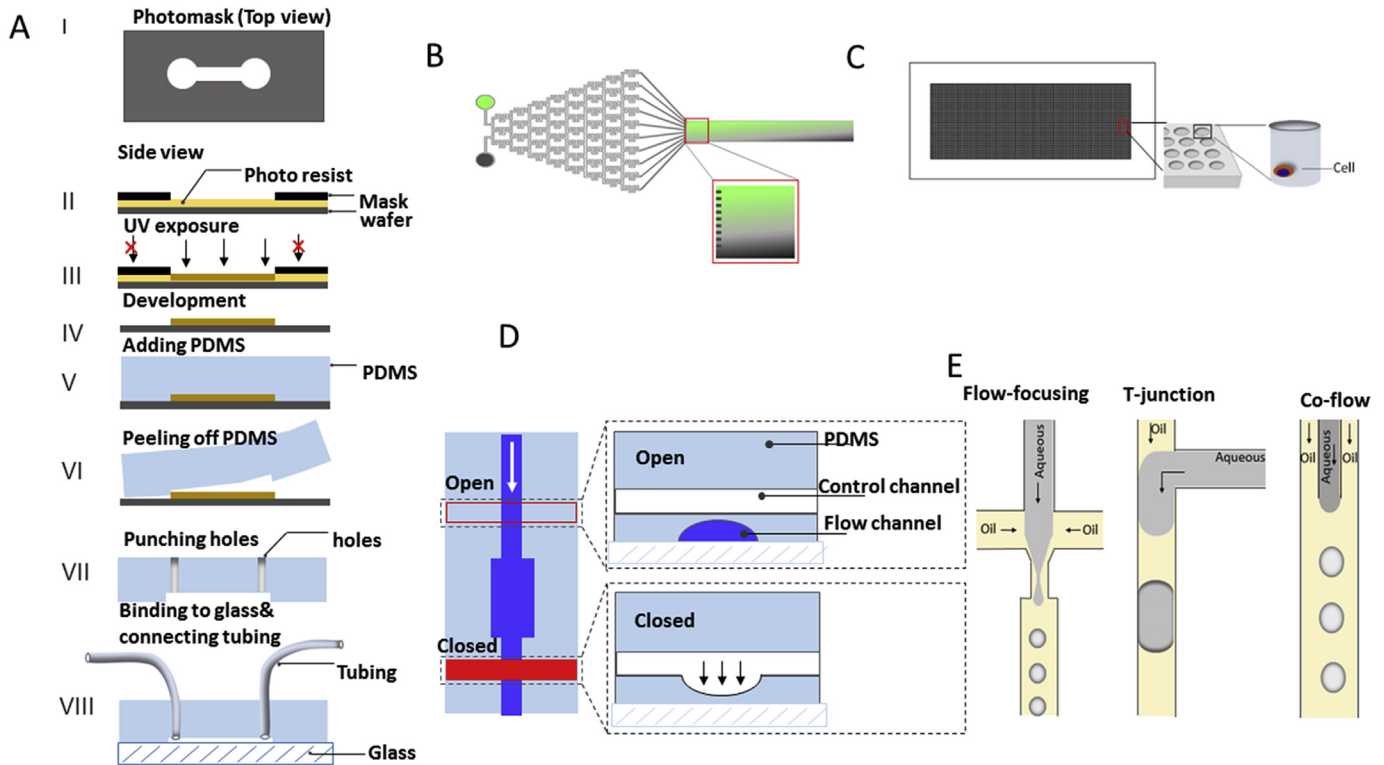
Fig. 2. Microfluidic technology. (**A**) Production of microfluidic chips by soft lithography. A photomask is generated using a computer-aided design (CAD) program (I). Subsequently, the pattern is projected onto a silicon wafer (gray) coated with a photosensitive polymer (yellow, II). The area exposed under UV light is polymerized as indicated in light brown, while the area masked by the photomask is not polymerized (III) and can be removed during development (IV), resulting in a mold that can be filled with an elastomer (V), typically polydimethylsiloxane (PDMS, light blue). After polymerization, the cured PDMS is peeled off (VI) and inlets and outlets are punched into the polymer (VII). Subsequently, the polymer structure is bound to a surface (typically glass, VIII) by plasma treatment, thus closing the channels. After that, tubing can be inserted into inlets and outlets to connect microfluidic channels to syringes filled with reagents. (**B**). Schematic of a gradient generated by microfluidic continuous flow. A reagent (e.g. fluorescein; top left) and a buffer (bottom left) are injected into two parallel inlets of the chip. Exploiting laminar flow and "Christmas tree" geometries this results in stable gradients within the cell chamber (right). (**C**). Schematic of thousands of nanowells molded in polydimethylsiloxane (PDMS) slides. Individual cells can be deposited in individual nanowells allowing researchers to do single-cell based assays. (**D**) Schematic of valve-controlled microfluidic channels. (Left panel) Channels highlighted in blue are microfluidic channels, controlled by valves indicated by a solid red rectangle (closed valve) or an empty red rectangle (open valve). (Right panel) Zoomed-in images of the valves which normally consist of two layers of channels perpendicular to each other. The upper channel is a control channel and the bottom channel is the channel in which reagents flow. To close the valve, air is injected into the control channel and the deformable PDMS layer between two channels is pushed down to block the bottom channel. To open the valve, pressure is released from the control channel so the deformable PDMS layer can be restored to its original position. (**E**) Aqueous droplets surrounded by oil can be generated using flow-focusing geometries, a T-junction or co-axial capillaries. (For interpretation of the references to colour in this figure legend, the reader is referred to the web version of this article.)

2. Immune signaling

The study of immunology and immunity is crucial both for the development of therapeutics, including vaccines, antibodies and drugs, and in the understanding of diseases, such as (auto-)immune diseases, aging and cancer. The plethora of cell types involved in immunity, coupled with frequent and complex interactions between different cells, makes the study of immunology particularly challenging.

With the development and improvement of flow cytometry, researchers have been able to better separate and distinguish different immune cell types, yet within any such category, there remains further heterogeneity. For example, single-cell transcriptomics performed on bone marrow dendritic cells (BMDCs) exposed to lipopolysaccharides revealed heterogeneity in gene expression and splicing (Shalek et al., 2013). In addition, within immune cell types, there are rare cell populations that have only recently been identified with single-cell technologies. For example, Mahata et al. recently discovered a steroid-producing subpopulation of CD4$^+$ T-helper 2 cells by single-cell sequencing technologies (Mahata et al., 2014). Furthermore, the distinction between different groups of cells may actually be more dynamic than

previously anticipated. For example, it was thought that the CD4$^+$ T-helper Th1 and Th2 lineages were distinct and mutually exclusive, and that any Th1/Th2 intermediates were unstable (Kaiko et al., 2008). However, a recent paper by Piene et al. showed that a highly stable Th1/Th2 intermediate cell type exists *in vivo* (Peine et al., 2013). This illustrates that the static views obtained from previous technologies measuring averaged population data may not be a true reflection of the dynamic nature of cells in the immune system. Therefore, to completely and thoroughly understand the state of the immune system, one must study single cells, and must be able to take measurements over space and time. The high spatiotemporal control made possible by microfluidic-based technologies helps to further improve our understanding of immune signaling, migration and cell-cell interactions.

2.1. Immune cell activation and responses

Immune cell activation is crucial in enabling specific immune cells to carry out their functions at appropriate locations and time points. These include the activation of antigen-specific T-cells in response to immune challenges (Malissen et al., 2014), the activation of natural killer (NK) cells in response to cellular stress (Chan

et al., 2014), and the activation of macrophages in the presence of microbial challenges (Mosser and Edwards, 2008). Standard assays utilized in monitoring immune cell activation and responses frequently only measure a few parameters and assume cell homogeneity, thus implicitly averaging responses that arise from populations that are actually highly heterogeneous. For example, ELISPOT (enzyme-linked immunospot) enables the detection of cytokines, which are captured by immobilized antibodies on a nitrocellulose membrane, and these are visualized by the addition of enzyme-coupled antibodies (Fig. 3A) (Crough and Khanna, 2009). This technique can only measure a few parameters at a time, and can only study bulk populations. Another technique

utilized is intracellular cytokine-assisted analysis, where intracellular cytokines after cell stimulation can be detected using flow cytometry (Fig. 3A). Protein transport inhibitors that prevent cytokine secretion are added, resulting in cytokines being trapped in Golgi/ER bodies, and these can be detected with fluorescently-labelled antibodies following cell permeabilization. Even as this enables the detection of single cells, intracellular cytokine-assisted analysis is limited by the number of fluorescence markers that can be utilized (Schmidt et al., 2013). For both these technologies, it is difficult to isolate cells for further molecular or gene expression analyses, and they frequently require pre-existing knowledge of immune cell responses, in order to know what cytokines to detect
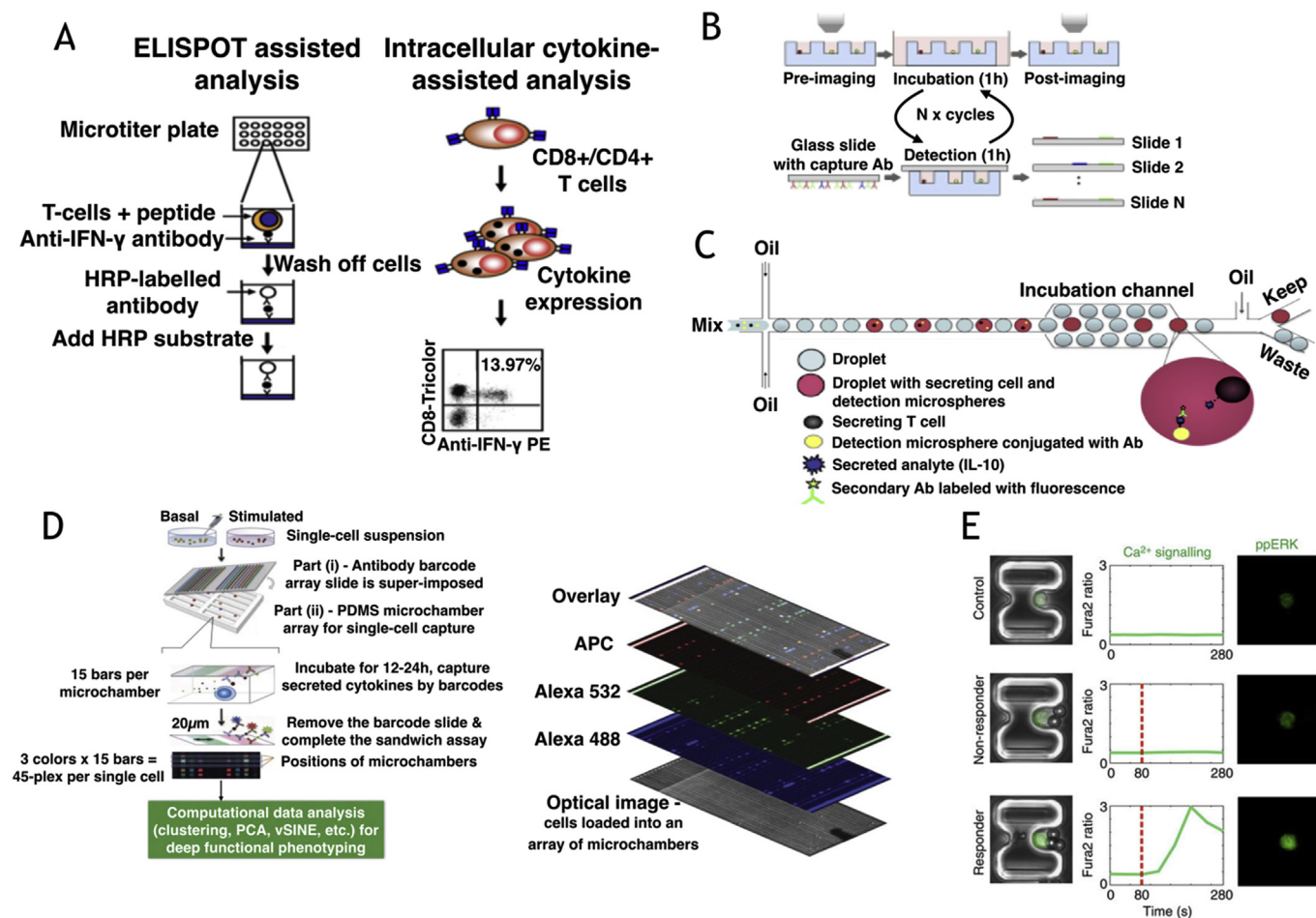
Fig. 3. **Studying immune cell activation.** (A) Standard assays used to study immune cell activation. (Left panel) For the ELISPOT assay, cells of interest are seeded in wells of microtiter plates that are coated with antibodies against the protein of interest (IFN-γ). The protein of interest, if present, will bind to the antibody. Cells are then removed, and proteins are visualized by the addition of a HRP-labelled antibody and subsequent addition of HRP substrate. (Right panel) Immune cell activation can be analyzed with flow cytometry, by incubation of the cells with protein transport inhibitors to prevent cytokine secretion and fluorescently-labelled antibodies against the cytokines of interest. Flow cytometry is then used to analyze cytokine levels. Reproduced from (Crough and Khanna, 2009). Amended with permission from American Society for Microbiology. (B) Nanowells can be used to detect multiple cytokines from single immune cells after activation. Single cells are placed into nanowells and imaged. Secreted molecules can be captured by the addition of a glass slide lid containing antibodies against molecules of interest. The lid can be removed and replaced at specific timepoints, enabling monitoring over time. Reproduced from (Han et al., 2012). (C) Droplet microfluidics can be used to detect secretion of cytokines by single immune cells. Droplets are generated from a mixture containing immune cells, detection microspheres with capture antibodies against the cytokine of interest and fluorescent detection antibodies. If the droplet contains a secreting cell and a detection microsphere, the cytokine is captured on the bead, and the fluorescent detection antibodies bind, resulting in localized fluorescence on the bead surface. Such droplets can be sorted for and further studied. Reprinted from (Konry et al., 2011), Copyright (2011), with permission from Elsevier. (D) Microchips can be used for highly multiplexed detection of cytokines and proteins. (Left panel) Single-cell suspensions of differentially-treated cells (basal and stimulated) are loaded into a PDMS microchamber array for single-cell capture (ii), before the antibody barcode array slide is superimposed (i), and the cells are incubated for 12–24 h. Each micro chamber has 15 bars, with 3 different types of antibodies in each bar, enabling the detection of 45 different proteins. After incubation, the barcode slide is removed and a sandwich assay is carried out. The slide is then imaged and the data further processed. (Right panel) An optical (brightfield) image, fluorescence images corresponding to the three different fluorescent dyes and the image overlay are shown. Reproduced from (Lu et al., 2015). (E) Studying T-cell activation using cell traps. Single immune cells were immobilized in the cell traps, and subsequently stimulated with anti-CD3/CD28 antibody-coated beads. Cytosolic Ca2+ levels were studies by monitoring Fura-2 levels. Cells were fixed 200s after stimulation and ERK phosphorylation was studied by on-chip staining and imaging. Time of pairing of beads with cells is indicated (red dotted line). Reprinted by permission from Macmillan Publishers Ltd: Nature Communications (Dura et al., 2015)., copyright (2015). (For interpretation of the references to colour in this figure legend, the reader is referred to the web version of this article.)

(Phetsouphanh et al., 2015). In addition, the fact that these methods only allow cytokine measurements means that they fail to assay other aspects of activation. The methods also have poor spatial (within-cell) and temporal resolution. Given that immune cell activation and the subsequent response is typically extremely rapid (in the range of seconds), optimal techniques should allow activation and response to be studied in real time. The high level of complexity and heterogeneity requires single-cell measurements, ideally in a multiplexed fashion monitoring multiple variables simultaneously. Optional isolation of particular single cells for further downstream assays, such as single-cell sequencing, is also highly desirable. These features can be achieved using microfluidic technology as discussed in this chapter: The use of small volumes means that secreted molecules from a single cell quickly reach detectable concentrations. In addition, a high degree of multiplexing is often possible, enabling a more thorough understanding of the complex processes involved in immune cell activation.

The Christopher Love lab has utilized nanowells to capture single cells, such as T-cells (Fig. 3B), to study their activation (Han et al., 2012). After loading, secreted molecules can then be captured by the addition of a glass slide lid containing antibodies against cytokines of interest. The lid can be removed and replaced at specific time points, enabling the monitoring of these cytokines over time. Han et al. measured the secretion rates of three cytokines (IFN-γ, IL-2, and TNFα) every two hours after stimulation, and eight distinct CD3$^+$ T-cell subsets could be distinguished more accurately than with merely timing of activation or the cumulative cytokine response. In addition, the dynamic study of cytokine release revealed that cytokine responses appear to follow largely deterministic courses, suggesting robustness within the system.

As an alternative to nanowells, droplet microfluidics can be utilized to detect cytokine secretion from single cells. Konry et al. encapsulated primary T-cells into aqueous droplets with beads conjugated to anti IL-10 antibodies (Konry et al., 2011). Secretion of IL-10 by T-cells could be detected by localized fluorescence on the bead surface. Coupled with fluorescence-based sorting systems (Xi et al., 2017; Frenzel and Merten, 2017), such assays could be expanded to isolate cells showing certain levels of cytokine secretion for further analysis (Fig. 3C).

Similarly, Chokkalingam et al. co-encapsulated activated Jurkat T-cells and beads coated with antibodies against the cytokines of interest into agarose-gel droplets. Cytokines were captured on the surface of the beads upon incubation, and after subsequent gelling, secreted cytokines were detected via incubation with fluorescently-tagged antibodies and subsequent flow cytometry analysis (Chokkalingam et al., 2013). The study emphasized the heterogeneity of cell behavior in cytokine secretion, where almost 57% of all activated Jurkat T-cells secreted all three cytokines studied (IL-2, TNF-α, IFN-γ), yet 15% did not secrete any. However, for nanowells and droplets, the number of secreted factors that can be detected is limited by fluorescence detection. Only up to four different cytokines were studied using the nanowell method (Han et al., 2012), while for droplets, only three different cytokines were studied (Chokkalingam et al., 2013).

Highly multiplexed monitoring of different cytokines and proteins was first seen with the development of valve-based microchips (Fig. 3D). These chips are able to capture single cells in small microchamber arrays. Antibodies against the proteins-of-interest are immobilized on glass slides that are used to seal the chambers, and secreted proteins are subsequently detected using immuno-sandwich assays. Initial assays were able to detect a dozen different proteins (Ma et al., 2011), and studied both the inflammatory cytokines released upon lipopolysaccharide (LPS)- stimulation of human macrophages and differences between cytotoxic T-cells from healthy donors and individuals with metastatic melanoma. By combining spatial (location) and spectral (color) multiplexing, subsequent assays could detect up to 45 different proteins in a single assay (Lu et al., 2015) (Fig. 3D). Here, the response of macrophages to LPS stimulation was studied. Significant cell-to-cell heterogeneity of protein secretion was observed, emphasizing the importance of such single-cell studies. In addition, this work revealed new insights about the role of macrophage inhibitory factor (MIF) in influencing activation of LPS-induced cytokine production.

Microfluidic cell traps have also been utilized to study immune cell activation. The Voldman lab exploited traps to analyze early activation dynamics of CD8$^+$ cells, where calcium signaling and ERK phosphorylation were studied (Fig. 3E) (Dura et al., 2015). CD8$^+$ T-cells were stimulated by pairing with anti-CD3/CD28 antibody-coated beads. Cytosolic calcium signaling was studied using a specific fluorescence probe (Fura-2), while ERK phosphorylation was studied via fixation and on-chip immunostaining and imaging. They found that cells could be categorized into responder and non-responder cells, where non-responder cells acted in a manner similar to unpaired cells. Within responder cells, higher ppERK levels correlated with shorter onset times and higher integrated Ca^{2+} levels.

Junkin et al have developed an automated microfluidic system that is able to deliver complex dynamic inputs to single immune cells, and monitor multiple outputs, including transcription factor activity and cytokine secretion over time (Fig. 4) (Junkin et al., 2016). Single cells were held in 40 isolated chambers, and valves were utilized to introduce dynamic and multiplexed inputs. The system contained 16 reagent inputs and an on-chip peristaltic pump, enabling the stimulation of cells with combinatorial or time-varying inputs. Cells were imaged in real time to monitor fluorescence-based readouts, migration and morphology. Cytokine secretion could be measured at different time points with an on-chip bead assay (Fig. 4): Antibody-bound beads were loaded into chambers in the lower half of the chip, and could be transported into a binding chamber via the use of peristaltic pumps. During binding, media from the cell chamber was pumped into the binding chamber, and mixed to allow cytokine binding. The beads were then rinsed and returned to their storage chambers, where cytokine concentrations were determined by immunosandwich assays. Subsequently, cells could be subjected to on-chip immunostaining, isolated for cell culture and expansion or isolated for gene expression analysis. Junkin et al. utilized this system to study single macrophages upon stimulation with bacterial lipopolysaccharide (LPS) with different dynamics, namely a single pulse, repeated pulses and continuous exposure, while measuring NF-κB and TNF secretion. They obtained an expected heterogeneity in cell responses, but found a lack of correlation between the relative amplitude of NF-κB and TNF levels in single cells. Computational modeling supported this finding, and instead suggested that TNF secretion was strongly correlated with TRIF activity. This example nicely illustrates the ability of microfluidic systems to measure multiple variables over time, at the single-cell level, while allowing multiple dynamic inputs, enabling one to gain highly multiplexed information about immune cell activation and responses in spite of noise and heterogeneity between single cells.

2.2. Cell-cell interaction

Immune cells do not exist alone, and many interactions are crucial in priming or activating immune cells to further fulfill their function. It is desirable to observe and even spatially and temporally control the events leading up to the interaction, and to then observe and quantify events that happen after interaction. High levels of control are crucial to disentangle complex signaling
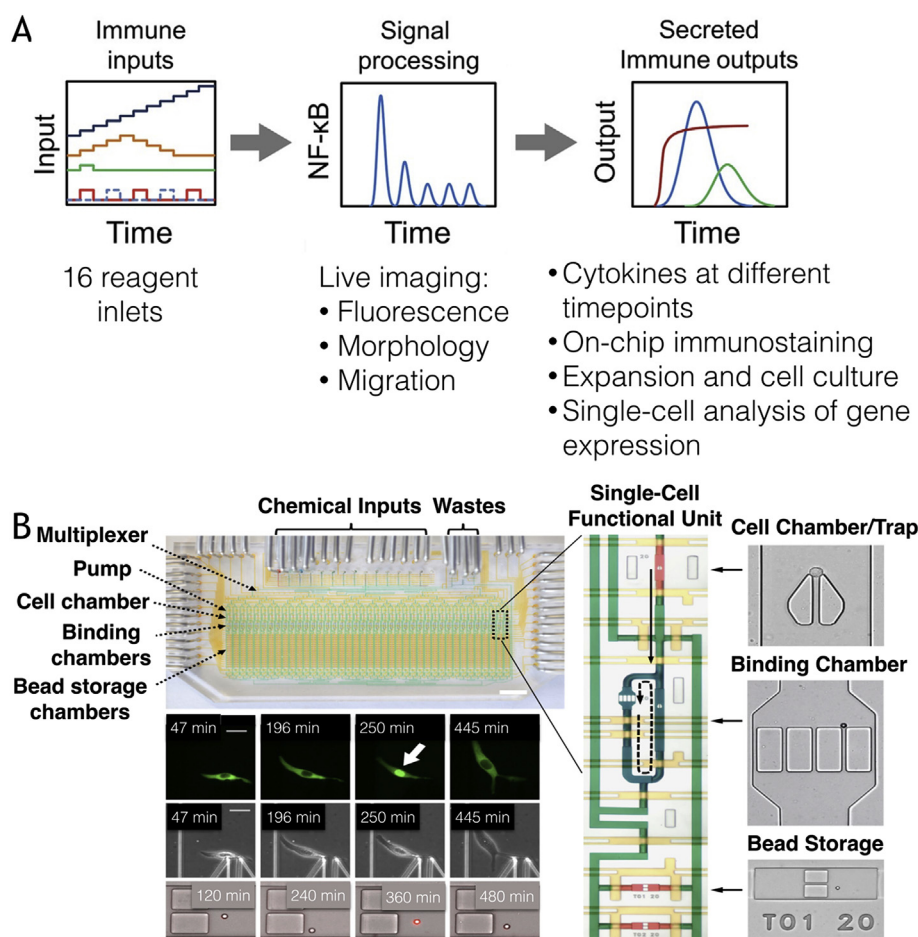
Fig. 4. Studying immune cell activation with multiple different inputs and outputs. (A) Multiple immune inputs with different dynamics are possible and live imaging of the cells can provide information on signaling (via the use of fluorescent markers or reporters), morphology and migration. Other possible outputs include cytokine levels at different timepoints, protein levels and localization (by on-chip immunostaining) and single-cell analysis of gene expression. In addition, cells can be extracted and further cultured. Adapted from (Junkin et al., 2016). (B) (Top left) The valve-based microfluidic device is shown, in which 40 single cells can be trapped and analyzed. The scale bar represents 5 mm. (Middle) A single-cell functional unit is shown and the arrows represent the movement of media during sampling (solid arrow) and media circulation to enable binding of cytokines to beads (dashed arrow). (Right) Microscope images of the different chambers are shown, namely the cell chamber/trap (top red), the binding chamber (blue) and bead storage chambers (bottom red). (Bottom left) Imaging of NF-kB activation is shown. Fluorescence images (top row) indicate RelA levels and localization, phase contrast images (middle row) and brightfield-fluorescence merged images of beads (bottom row) are shown. The scale bar represents 20 μm. The white arrow indicates activation of the cell (RelA in nucleus) while the red spot indicates detection of secreted proteins with a fluorescence immuno-sandwich assay. Reprinted from (Junkin et al., 2016). (For interpretation of the references to colour in this figure legend, the reader is referred to the web version of this article.)

events, to identify key players and elucidate the true order of events. As before, the high heterogeneity observed amongst immune cells and the will to analyze the kinetics of these interactions makes it desirable to have single-cell studies.

Before the use of microfluidic assays, immune cell-cell interactions were studied using bulk assays; immune cells were co-cultured and activated, then spun down to enable interaction, before being resuspended and assayed at specific time points (Fig. 5A) (Lee et al., 2002). These assays average the responses within the population and fail to account for heterogeneity. In addition, any detected responses may be induced by one or multiple other cells, but these bulk assays cannot control or detect the ratio of cells involved in such interactions.

Droplet-based microfluidics has also been utilized to examine immune cell interactions (Fig. 5B) (Sarkar et al, 2015, 2016). Different cells were co-encapsulated, and their interactions monitored by imaging. In Sarkar et al (2015), T-cells were co-encapsulated with activated dendritic cells (DCs), and T-cell calcium levels were monitored using Fluo-4, which enables monitoring of calcium levels via fluorescence microscopy (Sarkar et al.,

2015). The authors found an increase in T-cell calcium levels in both directly interacting DC-T-cell pairs and in cases where no contact was made between DCs and T-cells present in the same droplet, potentially reflecting contact-dependent and independent processes. In addition, Sarkar et al (2016) further studied the interactions between T-cells and DCs (Sarkar et al., 2016). They found that non-activated DCs interacted less, and more transiently with T-cells, while chemokine-loaded DCs had longer and more stable interactions with T-cells. In addition, by studying droplets in which there were more than one cell of either type, they found that a single DC could interact with more than one T-cell but not vice versa. They also studied the interaction between CD8^{+} T-cells and RPMI-8226, a multiple melanoma cell line, and assessed target death by the loss of Calcein-AM fluorescence, which indicates a loss of membrane integrity. They discovered two classes of different phenotypes; fast and slow killing, and found that IFN-c plays an important role in fast killing.

Cell-cell interaction can also be studied with cell traps, which enable the regulated and specific pairing of specific single cells. Dura et al. described a five step loading process (Fig. 5C) which
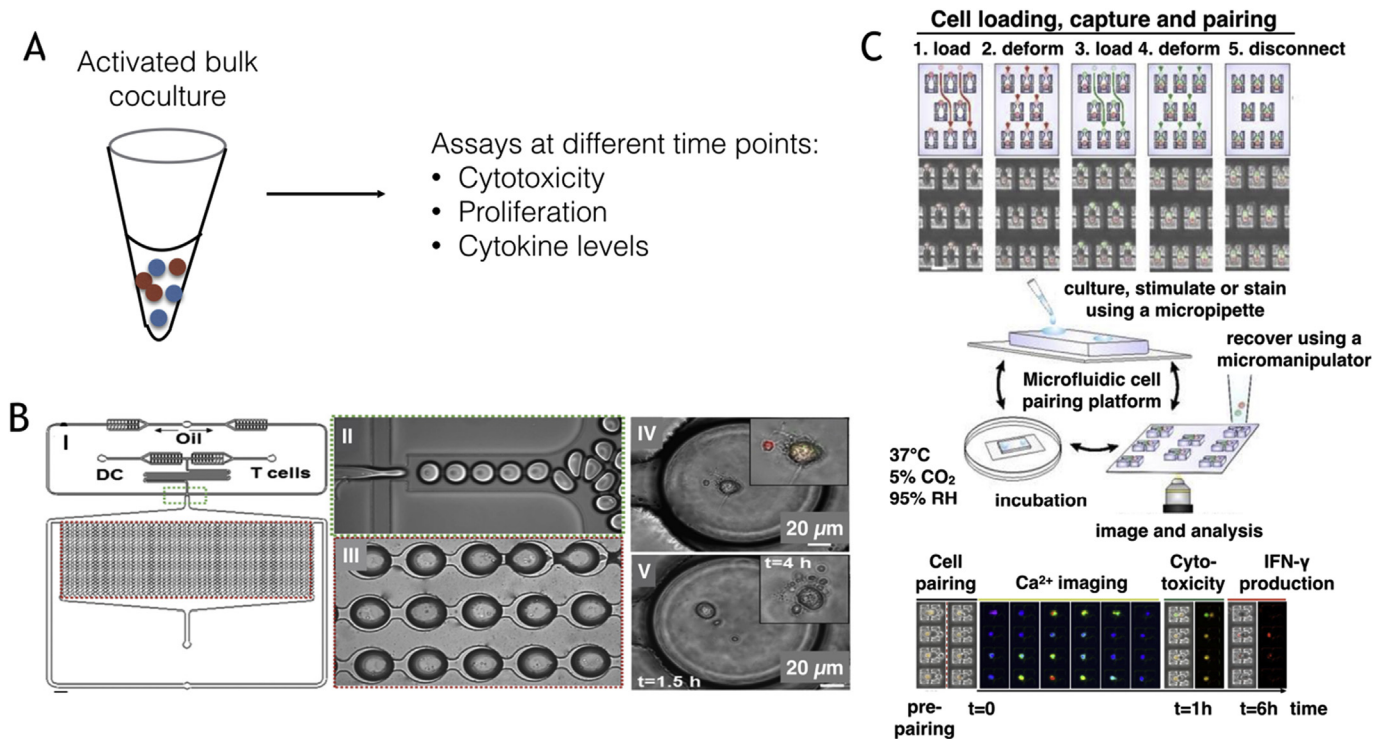
Fig. 5. **Examining immune cell-cell interactions.** (**A**) Immune interactions are assayed at a bulk population level by activating the cells and briefly spinning them down to induce interactions. Various assays, such as those to detect cytokine levels and those for cytotoxicity or proliferation are then carried out. (**B**) Co-encapsulation of different single cells by droplet microfluidics can be used to study immune cell-cell interactions. (I) A schematic of the overall droplet microfluidic system is shown, where oil, dendritic cells and T-cells are introduced in separate inlets. (II) Droplets are generated in a flow-focusing geometry. (III) Droplets are held in a docking array for imaging. (IV) A dendritic cell (DC) and a T-cell in a droplet can be seen, with the inset showing dendritic extensions. (V) Cellular exocytosis was also observed in the droplet, with the inset showing the vesicles secreted by the DC. Reprinted from (Sarkar et al., 2016), with the permission of AIP Publishing. (**C**) Cell traps can be utilized to study cell-cell interactions. (Top panel). A five step cell loading process is illustrated, where cells of the first cell type (red) are captured in the cell traps (1) and transferred into the larger trap by flow-induced deformation (2). The second cell type (green) is loaded in a similar manner (3, 4). (Middle panel) Fluidic connections are removed to enable movement of the chip for further incubation, imaging or subsequent recovery. (Bottom panel) A multitude of variables were monitored (bottom panel), including Ca^{2+} levels for 45—60 min upon cell pairing (t = 0), cytotoxicity at t = 1 h and IFN-γ production at t = 6 h. Reproduced from (Dura et al., 2016). (For interpretation of the references to colour in this figure legend, the reader is referred to the web version of this article.)

enabled the deterministic formation of interactions at controlled time points, and at a controlled 1:1 cell ratio (Dura et al., 2015). Cells of different cell types were sequentially loaded into traps and these used to keep the individual cell pairs in place, maintaining the cell-cell interactions and enabling the acquisition of information via imaging over time. The media surrounding the traps could also be easily exchanged without disturbing the interacting cells. With this system, Dura et al. investigated the early activation dynamics of CD8$^+$ cells, upon interaction with antigen-loaded B cells. They measured cytosolic calcium mobilisation for both the B and T cells, CD8 co-receptor expression on the T-cell surface and pMHCI and MHCII-eGFP on B cells. By sequentially stimulating the cells, first by pairing with antigen-loaded B cells, and then with ionomycin, they found different categories of cells based on how they responded to the stimulation, namely double responders (that responded to both stimulations), single responders (which responded to only ionomycin activation) and non-responders. The use of antigenic peptides with different TCR affinities enabled a population-wide study to examine how the heterogeneity of the population varied. The system was also utilized to study CD8$^+$ T cells from mice that recognize the same epitope, but with different affinities. They were able to corroborate the hierarchy of cytokine secretion and to illustrate at which point the signaling of the low affinity T-cells differed from the high affinity ones. In a subsequent paper, they also demonstrated other important parameters via on- and off-chip culture, imaging, staining and single-cell gene expression analysis (Dura et al., 2016). The interaction between natural killer (NK) and

tumor cells was investigated, by examining real-time calcium response and cytotoxic activity using a cell-permeable fluorogenic granzyme B substrate. In addition, IFN-γ levels were studied by intracellular cytokine staining on chip. They found an expected heterogeneity between the different single cells, and their data further suggested an inverse link between cytotoxicity and IFN-γ production, which are two different effector functions of NK cells. Their work also suggests that early calcium signaling affects cytotoxicity and IFN-γ production.

In summary, microfluidic technology enables specific and highly-regulated cell pairing at a single-cell level, with the possibility to measure various variables over time both on- and off-chip. This enables a more thorough investigation of early signaling events between interacting cells, and furthers our understanding of immune cell-cell interactions.

However, the ability of these *in vitro* microfluidic studies to truly recapitulate the *in vivo* immune niche has not yet been demonstrated. The development, maturation and survival of immune cells is highly dependent on many other cell types, cytokines and proteins, that together provide a specific niche. For example, the bone marrow plasma cell survival niche, which enables the continued production of antibodies by plasma cells, is maintained by a multitude of different cell types, including stromal cells and eosinophils (Chu et al., 2011). It has not yet been shown that these complex environments can be successfully recreated on chip, but the controlled microfluidic *in vitro* environment at least allows to study individual parameters of immune cells and their interactions

in great detail.

3. Immune cell migration

Immune cell migration is crucial in the functions of many immune cells, such as T-cell migration in searching for antigen-presenting cells (Krummel et al., 2016), inflammation and wound-healing.

Traditionally, time-lapse imaging has been used to study single migrating immune cells *in vivo* (Beltman et al., 2009). These observation-based studies have revealed much about cell movements *in vivo*, but the lack of manipulation makes them limited in revealing the exact dynamics and factors that affect migration. In contrast, microfluidic technologies enable the generation of specific gradients and geometries, to study immune cell migration in an easily manipulatable *in vitro* setting. Such systems typically aim to mimic some aspect of the tissue microenvironment, to recreate certain aspects of *in vivo* migration. This enables elucidation of the

specific factors regulating migration in real time, while changing individual parameters of interest.

Microfluidic chips can be used to generate simple chemokine gradients for chemotaxis assays (Fig. 6A). For example, human peripheral blood T-cells were placed in a microfluidic chip and subjected to single or competing gradients of the chemokines CCL19 and CXCL12 (Lin and Butcher, 2006), and chemotaxis was observed via imaging of the cells at different time points. The authors showed that the T-cells migrate towards the individual chemokine gradients, but that in a competing gradient of CCL19 and CXCL12, a slightly higher percentage of cells appeared to migrate towards the CCL19 gradient. The initial position of the cell in the channel affected this movement, where a higher percentage of cells in the side of the channel closer to higher CCL19 levels migrated to CCL19, compared to cells in the other side.

Other microfluidic assays have similarly studied the relative importance of different cytokine gradients in attracting various immune cell types. For example, Ricart et al. showed that CCL19 is
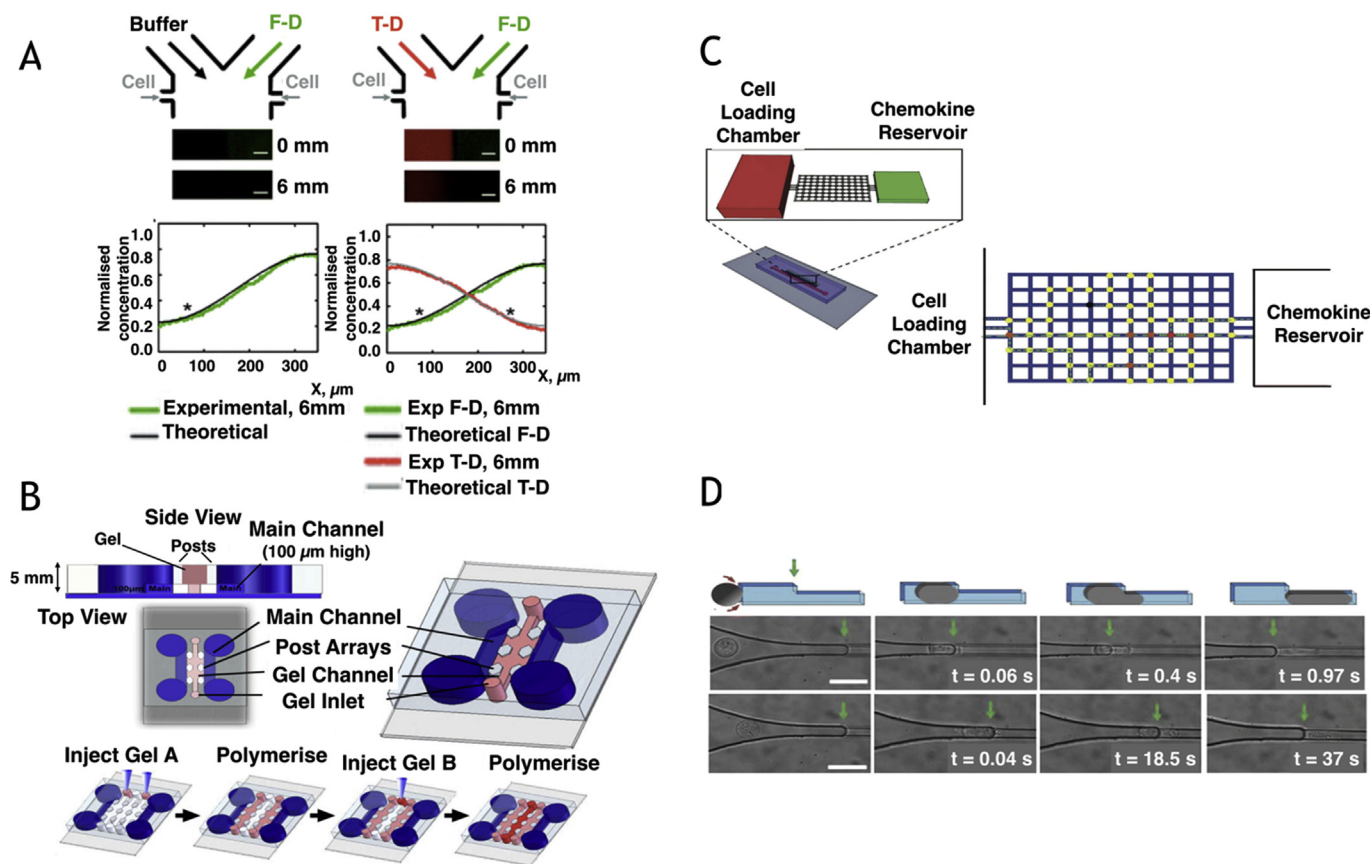
Fig. 6. Studying cell migration and physical properties. (**A**) Generation of simple chemokine gradients with continuous flow microfluidics. Gradients of a single chemokine (left) or of two opposing chemokines (right) can be generated. (Top panel) A diagram of the microfluidic setup is shown. Buffers are flowed from the top, while cells are added from either side. (Middle panel) Fluorescence micrographs of FITC-Dextran (F–D) (A) and FITC-Dextran (F–D) and Texas-Red-Dextran (T–D) (B) at 0 mm and 6 mm below the Y-junction are shown. The scale bars represent 50 μm. (Bottom panel) The experimentally measured gradient profiles at 6 mm and the theoretical profiles are in agreement. Reproduced from (Lin and Butcher, 2006) with permission of The Royal Society of Chemistry. (DOI: https://doi.org/10.1039/b607071j) (**B**) Hydrogels with properties resembling tissues can be added to microfluidic chips used to study immune cell migration. (Top panel) Schematic of a chip design, where the main channels for the infusion of media and nutrients are separated by a gel that optimally resembles tissue, in which cells can be added. (Bottom panel) Chips can be made with multiple hydrogel layers, optionally with different properties. The first gel is injected into the inlets and left to polymerize, before this is repeated for subsequent gels. Reproduced from (Huang et al., 2009) with permission of The Royal Society of Chemistry. (DOI: https://doi.org/10.1039/b818401a) (**C**) Schematic of complex maze geometry used to study T-cell migration patterns. Cells are loaded at one end of the maze with a chemokine reservoir at the other end. Reproduced from (Jain et al., 2015) with permission of The Royal Society of Chemistry. (DOI: https://doi.org/10.1039/c5ib00146c) (**D**) Microfluidic device for the assessment of leukocyte stiffening. (Top panel) A schematic of the assay is shown. Leukocytes are pulled into the channel via suction, while being followed by video microscopy to study leukocyte stiffness. (Middle and bottom panels). Video microscopy was used to follow leukocytes that were subjected to a local suction pressure of ΔP = 160 Pa, after a 1 h incubation with serum from a healthy individual (middle panel) or of a patient with moderate to severe acute respiratory distress syndrome (ARDS) (bottom panel). The green arrows indicate the entry of constriction C2, and the scale bar represents 20 μm. Reprinted from (Preira et al., 2016), under the Creative Commons Attribution 4.0 International License (http://creativecommons.org/licenses/by/4.0). (For interpretation of the references to colour in this figure legend, the reader is referred to the web version of this article.)

better at attracting dendritic cells than CCL21 or CXCL12 (Ricart et al., 2011a). However, in a three-dimensional extracellular matrix, it was shown that cells preferentially migrate towards a CCL21 gradient over a CCL19 gradient (Haessler et al., 2011). Nandagopal et al. also showed that a combined field of CCL19 and CCL21 repels T-cells instead of attracting them, showing how such cytokine signals may interact to generate more complex responses (Nandagopal et al., 2011). Migration can not only be detected by direct imaging, but also via mechanical stimulation of fluorescently-labelled micropost arrays (Ricart et al., 2011a, 2011b). Dendritic cells exert a force when migrating above these micropost arrays, and the direction of movement can be detected via the tilting of the microposts. This enables further understanding of the mechanics of dendritic cell migration.

As immune cells frequently migrate through tissues, these microenvironments should be taken into account in studies of immune cell migration. Layers of 3D hydrogels of specific geometries have been used to model these microenvironments, and these assays monitor migration and cell-cell interactions in real-time (Fig. 6B) (Huang et al., 2009; Haessler et al., 2011). Huang et al. showed that RAW macrophages were able to invade neighboring gels containing breast cancer cells, but were less invasive in gels lacking cells (Huang et al., 2009). More complex geometries can also be modeled using microfluidics: In order to study T-cell exploration patterns, Jain et al. designed a microfluidic chip containing a maze design mimicking a tissue-like environment (Fig. 6C), and introduced a chemokine gradient across the maze (Jain et al., 2015). By quantifying the migratory patterns of lymphocytes through the maze, they found that cell activation and the presence of chemoattractant gradients generally increases cell exploration. The tightly regulated geometrical and chemical features enabled precise measurements and quantification of migration. More complex mazes have also been utilized to assess neutrophil decision-making: Ambravaneswaran et al. showed that in complex maze-like channels leading to chemoattractant sources, neutrophils are able to select the most direct route (Ambravaneswaran et al., 2010).

In addition, microfluidic systems can also be used to assess the physical properties of immune cells, which sheds light on the natural functioning of immune systems. For example, in Preira et al., sera of healthy individuals or that of patients with early acute respiratory distress syndrome (ARDS) was added to leukocytes, before assessing how long these leukocytes took to enter a microfluidic channel containing a constriction (Fig. 6D) (Preira et al., 2016). They found an association between leukocyte stiffening and ARDS disease severity, and that this stiffening was largely induced by increased levels of certain cytokines (IL-Iβ, IL-8 and TNFα). This enables a further understanding of the disease and the technology could potentially be exploited for the discovery of therapeutics.

The freedom of design of microfluidic chips enables the generation of many different geometries that can be used to model possible geometries involved in immune cell migration. In addition, the ability to generate and regulate chemokine gradients enables one to better elucidate the exact factors and causality seen in immune cell migration.

4. Phenotypic screens for antibodies with desired properties

Since monoclonal antibodies were first described some 40 years ago (Kohler and Milstein, 1975), they have opened the door to a new era of basic research and clinical therapeutics. Monoclonal antibodies are invaluable research tools and the fastest growing class of all new drugs with sales of more than 75 billion USD in 2015. They have gained major importance in the treatment of infectious diseases (Casadevall et al., 2004; Kotsovilis and Andreakos, 2014; Qiu et al., 2014), cancer malignancies (Carter, 2001; Strait et al., 2015; Sliwkowski and Mellman, 2013) and inflammation (Chan and Carter, 2010). To date, there are 34 FDA approved therapeutic antibodies in clinical use. Monoclonal antibodies can be screened very efficiently for binding using phage display and related technologies (Hoogenboom, 2005). However, binding alone is not sufficient; therapeutic antibodies must also modulate (typically inhibit) the activity of the target, whereas these methods select only for binding to a drug target and not for inhibition of its function. To overcome this limitation, functional antibody screens are typically carried out using hybridoma cell technology (Nelson et al., 2010; Little et al., 2000). In this approach, laboratory animals are immunized with the antigen of interest before antibody-releasing B-cells are isolated from the spleen. These B-cells are then rendered immortal by fusion with myeloma cells, diluted to generate microtiter plate wells containing single cells and expanded to form clonal populations. Subsequently, the supernatant of each population can be tested to screen for the desired activity. However, the need for clonal cell expansion (to obtain detectable concentrations of antibodies), and hence cell immortalization, typically limits the number of clones that can be screened to no more than a few thousand. This represents only a tiny fraction (approximately $1/10^4$) of the available antibody repertoire in a mouse. Furthermore, fully matured bone marrow plasma cells (BMPCs), which secrete the vast majority of high affinity IgGs in the blood stream, are not suitable for hybridoma cell generation as they cannot be cultivated outside their natural niche (Reddy et al., 2010). As a consequence, hybridoma technology is only of limited use for efficient, high throughput screening of therapeutic antibodies. Significant efforts have therefore been put into alternative immortalization techniques, such as immortalizing B-cells using the Epstein-Barr virus (EBV) or genetic reprogramming (Traggiai et al., 2004; Kwakkenbos et al., 2010), but these methods are mostly applicable to human memory B-cells and/or are very time consuming and limited in throughput.

It is therefore obvious that methods for the direct screening of non-immortalized B-cells are highly desirable. This was first achieved using single cell PCR of FACS-sorted antibody-secreting plasma cells (ASCs) (Wrammert et al., 2008), yet this still required a secondary screen for binding specificity. Specific B cell populations, like memory B cells, express surface B-cell receptors and thus can be screened directly for binding affinity using fluorescently labelled antigens and subsequent FACS (Wu et al., 2010). However, this approach is restricted to binding assays. Primary B-cells have also been co-cultivated with antigen-coated beads or antigen-expressing cells in the presence of fluorescently-labelled secondary antibodies. B-cells secreting antibodies with desired binding properties then generate "fluorescent foci" in their direct vicinity and can hence be identified (Simon Tickle et al., 2009). In theory, this approach should also allow functional screens, but the specific isolation of positive secretors is very challenging and restricts throughput.

Microfluidic systems can overcome many of the limitations observed in bulk systems: Most of all, they enable assay volumes small enough to obtain detectable concentrations of antibodies from single primary cells. Using picoliter to nanoliter volumes, these can reach 0.1−1 μM, given an immunoglobulin secretion rate of approximately 5000 molecules/s for plasma cells and their derivatives (Hendershot et al., 2003). This can be exploited by cultivating B-cells in nanowells of 10−20 μm in diameter and in depth. Corresponding devices can be produced with a density of up to several hundred thousand wells per chip (Fig. 2C). Jin et al. performed a corresponding screen by coating nanowells with anti-immunoglobulin antibodies, enabling them to capture the
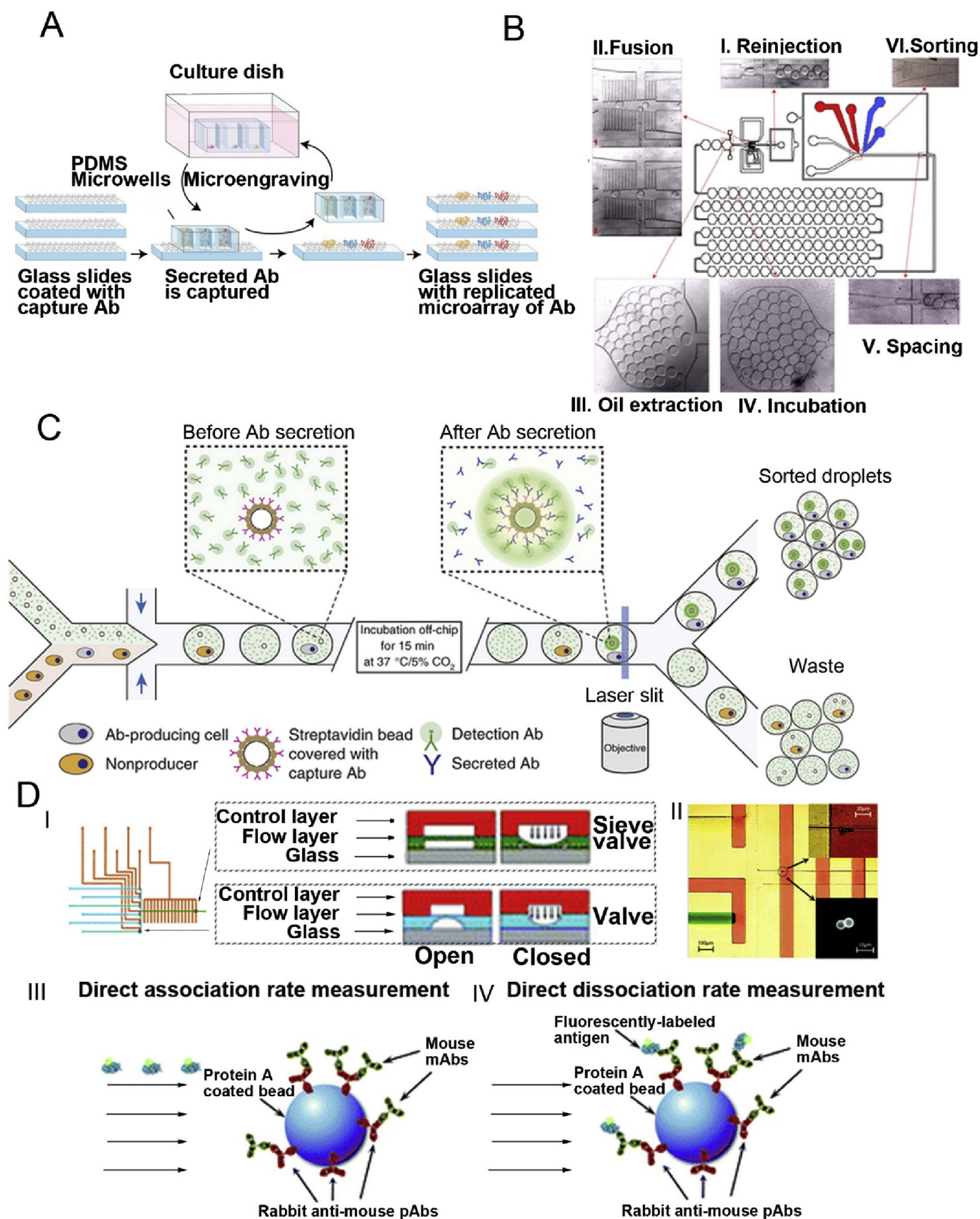
Fig. 7. Microfluidic antibody screening. (A) Schematic illustration of the nanowell technology utilized for antibody screening. Cells are seeded in the PDMS nanowell array at a density of approximately one cell per well. A glass slide coated with capture antibodies is then placed in contact with the PDMS nanowells and incubated for 30–60 min, enabling secreted antibodies to accumulate and be captured onto the surface of the glass slide. This process can be repeated several times to produce antibody microarray replicates sufficient

antibodies secreted by single B lymphocytes loaded into the nanowells (Jin et al., 2009). Subsequently, fluorescently-labelled hepatitis B antigens were added to stain antigen-specific B cells which were then isolated using a micromanipulator fitted with capillaries. Similarly, the secreted antibodies can also be captured on glass slides coated with anti-immunoglobulin antibodies placed on top of nanowells. The glass slide can then be rinsed, blocked and stained by fluorescent antigens for antibody screening (Love et al., 2006; Ogunniyi et al., 2009). In addition, the process can be repeated and multiple glass slides can be stained with either isotype specific fluorescent antibodies for antibody isotyping or a series of concentrations of fluorescent antigens for generating binding curves revealing antibody affinities (Story et al., 2008) (Fig. 7A). This approach enables rapid (~12 h), high-throughput (>100,000 individual cells per experiment) screening and characterization of antigen reactive antibodies. However, functional assays still have not been implemented in these systems.

Droplet microfluidic systems provide another alternative for antibody screening. Instead of compartmentalizing single cells in separate nanowells, they are compartmentalized in tiny aqueous droplets (~30–100 μm in diameter) surrounded by oil. A major advantage compared to nanowells is the fact that hits can be identified and isolated in an automated fashion using fluorescence activated droplet sorting. This enables the screening of hundreds of samples per second, overcoming the need for any slow mechanical equipment such as micromanipulators. Similarly, further reagents can be added to the samples (e.g. to initiate a fluorescence readout) at high throughput by droplet fusion. We have exploited these conceptual advantages in a functional screen for antibodies inhibiting the congestive heart failure drug target angiotensin-converting enzyme 1 (ACE-1) (El Debs et al., 2012) (Fig. 7 B). To demonstrate the power of the approach, we started with a heterogeneous hybridoma cell population in which only one in ten thousand cells secreted a well-characterized antibody (4E3 (Skirgello et al., 2006)) inhibiting ACE-1. After encapsulating individual cells into droplets, the resulting emulsion was incubated off-chip for 6 h to obtain significant antibody concentrations. Subsequently, the droplets were reinjected into a microfluidic device and fused with a second droplet species containing all components of a fluorescence assay for ACE-1 activity. In a further step, droplets with low fluorescence intensity (indicating ACE-1 inhibition) were sorted and the encapsulated cells were recovered and characterized off-chip. As expected, more than 90% of these cells expressed the 4E3 antibody (corresponding to a more than 9000-fold enrichment of cells expressing desired antibodies during a single sort) and even the selection of super secretors (cells expressing drastically increased levels of antibodies) was observed. The approach enabled the screening of more than 300,000 cells in a single experiment and should also be applicable to non-immortalized primary B-cells, as no cell proliferation is required. Similarly, droplet microfluidics can also be used to screen for specific binders (Mazutis et al., 2013), similar to fluorometric microvolume assay technology (FMAT, (Miraglia et al., 1999),) (Konry et al., 2011): For screening, antibody-secreting cells are encapsulated into droplets together with antigen-coated beads and secondary fluorescently-labelled antibodies. If the primary antibodies bind to the bead, the fluorophores of the secondary antibodies also get localized, resulting in a narrow high intensity fluorescence peak when these droplets pass the detector. However, if the primary antibodies do not bind to the target, the secondary antibodies remain homogeneously distributed, giving rise to a broad, low intensity fluorescence peak (Fig. 7C). Even though the screening of primary B-cells in droplets has not yet been published, it is just a matter of time until this format is routinely used for this purpose.

In addition to nanowells and droplets, antibody secreting cells can also be screened in valve-based systems. Singhal et al. have described a bead-based microfluidic assay that is capable of measuring antibody-antigen binding kinetics with a sensitivity comparable to surface plasmon resonance (SPR), on the single-cell level (Singhal et al., 2010). The technology utilizes valves to capture beads while still enabling fluid exchange (Fig. 7D). These beads were coated in Protein A, enabling the capture of antibodies-of-interest. Subsequent addition of fluorescently-labelled antigen enabled direct measurement of binding kinetics, while washing with unlabelled antigen, followed by fluorescently-labelled antigen enabled indirect measurement of these kinetics (Fig. 7D). Even though valve-based microfluidic chips are somewhat limited in the overall throughput (the number of chambers is much smaller than for nanowells or droplets; typically no more than maximally a few thousand), they provide a very high level of control, even enabling complex washing steps. Furthermore, the technology is quite robust and hence nicely complements the other formats.

Taken together, microfluidic approaches have significant advantages for phenotypic antibody screening: Operating on the single-cell level enables unprecedented throughput and overcomes the need for cell immortalization. A current hurdle for direct B-cell screening is the limited efficiency in the downstream sequencing of antibody encoding genes from single-cells (typically less than 50%), but this is continuously being improved using optimized protocols, similar to what is used in single-cell transcriptomics (Tang et al., 2009; Macosko et al., 2015).

to determine the specificity, isotype and affinity of the captured antibodies. Reproduced from (Story et al., 2008). (B) Droplet microfluidic technology for antibody screening based on inhibitory properties. Droplets are generated from a solution containing angiotensin converting enzyme 1 (ACE-1) and hybridoma cells expressing either the ACE-1 inhibitory antibody 4E3 or the non-inhibitory antibody Elec-403, and these droplets are incubated off-chip for 6 h to allow for efficient antibody production inside the droplets. Droplets (containing cells and ACE) are reinjected into an integrated microfluidic chip (I) and fused with droplets containing the fluorogenic ACE-1 substrate (II). Upon substrate addition, droplets containing 4E3 hybridoma cells exhibit lower fluorescence (than those with Elec-403 hybridoma cells) due to inhibition of ACE activity by 4E3. The droplets then pass through a delay line (IV), and are subsequently sorted for low fluorescence (VI), resulting in the specific collection of cells secreting ACE-1-inhibitory antibodies. Reproduced from (El Debs et al., 2012). (C) Droplet microfluidics for antibody screening based on binding assays. Antibody-producing and non-antibody producing cells (orange and gray respectively) are co-encapsulated together with green fluorescently–labelled goat detection antibodies (green) and streptavidin beads coated with goat anti-mouse-Fc capture antibodies (magenta). After incubation, beads present in a droplet with antibody-producing cells become highly fluorescent, as secreted antibodies are captured on the bead (by the anti-mouse-Fc antibodies), and green fluorescent detection antibodies bind to the captured antibodies in a sandwich assay. The emulsion is then re-injected into a second microfluidic chip for the specific sorting of, positive droplets. Adapted by permission from Macmillan Publishers Ltd: Nature Protocols (Mazutis et al., 2013), copyright (2013). (D) Valve-based technology used to assess antibody-antigen binding. (I) The device contains six flow channels (blue) which can be controlled by independent control valves (orange). Protein A beads coated with anti-mouse antibodies (similar to those shown in II; visualized by brightfield- (top inset) and fluorescence microscopy (bottom inset)) are loaded and trapped at the sieve valves (intersection of yellow and orange channels, II), alongside single mouse hybridoma cells. Antibodies released by the hybridoma cells are captured on the beads by the anti-mouse antibodies. Antibody-antigen binding kinetics are then measured by first washing with buffer, then introducing buffers with increasing concentrations of fluorescent antigen and imaging the beads at various time points, enabling the measurement of association and kinetics of antibodies released from the single hybridoma cells (III). Dissociation kinetics can be measured by flushing the chip with PBS buffer and imaging to measure the rate of antibody-antigen dissociation (IV). Adapted with permission from (Singhal et al., 2010). Copyright 2010 American Chemical Society. (For interpretation of the references to colour in this figure legend, the reader is referred to the web version of this article.)

5. Screening the B- and T-cell repertoire

In addition to screening B-cells on the phenotypic level, one can also exploit next generation sequencing (NGS) based approaches to infer information on antibody binding, an approach commonly referred to as "Ig-seq". Reddy et al. isolated bone marrow plasma cells (BMPCs: CD45R− CD138+) from immunized mice and amplified all antibody-encoding genes by PCR with well-characterized degenerate primers (Krebber et al., 1997). Subsequently, the samples were applied to NGS. Based on the sequencing data, they then paired the most dominant heavy (V_H) and light chains (V_L) according to their relative frequencies, and obtained 78% antigen-specific antibodies (Reddy et al., 2010). It was found that light chains show less diversity as compared to heavy chains, meaning that multiple pairings had to be generated and validated by measuring affinities.

Apart from antibody screening purposes, sequencing of the BCR repertoire has many more important applications: The B-cell receptor (BCR) is also key to understanding B cell clonal evolution during infection, vaccination, aging and in autoimmune diseases. Conventional approaches for interrogating the BCR repertoire rely mainly on the combination of FACS and single cell PCR followed by Sanger sequencing (Fig. 8A) (Wrammert et al., 2008; Tiller et al., 2008, 2009). However, these methods provide only a few hundred BCR pairs at most, giving just a small glimpse into the BCR repertoire with a potential diversity of more than 1×10^{13} for humans (Yaari and Kleinstein, 2015; Georgiou et al., 2014) and 1×10^{11} for mice (Pabst et al., 2015). With the advent of next-generation sequencing, complementarity-determining region 3 (CDR3) fragments from pooled isolated B cells of zebrafish have been sequenced, revealing unprecedented understanding of the immune system of an individual organism (Weinstein et al., 2009). Similarly, heavy or light chain genes of particular lineages from PBMCs of HIV-infected patients (Wu et al., 2011; Doria-Rose et al., 2014) have been sequenced by NGS, which allowed the study of elicitation and clonal evolution of particular broadly neutralizing antibodies during HIV infection and provided important insights into HIV-1 vaccine development. A major drawback of NGS on pooled B cells is the inevitable loss of endogenous pairing of heavy and light chain sequences, at least for clones of lower abundance (for which the frequency based pairing described above does not work). To take advantage of NGS for BCR repertoire sequencing but still retain the pairing information of heavy and light chain genes of single B cells, cell barcodes must be introduced to label individual B cells before pooling them together. A two-dimensional barcoded primer matrix with 240×192 tags, capable of barcoding over 46000 individual B cells, was developed and tested. As a result, from three 384-well plates of single sorted B cells of different subtypes, 33% (381/1152) cells yielded full length heavy and light chain genes (Busse et al., 2014). However, processing thousands of single cell PCR reactions in microtiter plates is very time-consuming, labor-intensive and consumes relatively high amounts of reagents.

This can be overcome by microfluidics, a powerful tool for increasing the throughput of single-cell PCR. For example, a microfluidic chip with 1.7×10^5 nanowells was developed in which single B cells together with poly(dT) magnetic beads can be deposited into individual wells. Cell lysis and mRNA capture can then be done in individual nanowells. Subsequently, magnetic beads annealed with mRNA from individual cells were pooled, washed and encapsulated into droplets together with components for RT-PCR and linkage PCR. After RT-PCR and linkage PCR, the emulsion was broken and V_H:V_L cDNA fragments of approximately 850 bp were recovered and analyzed by paired-end 2×250 Illumina MiSeq sequencing. Using this approach, a total of more than 5×10^4 lymphocytes could be analyzed at the single-cell level (DeKosky et al., 2013) (Fig. 8B). To further improve the throughput, an entirely emulsion-based technology was developed in the Georgiou lab: As a functional counterpart of microwells, millions of water-in-oil droplets encapsulated with single B cells, poly(dT) beads and lysis buffer were generated in one hour using a flow-focusing device. This allows the sequencing of a repertoire of over 2×10^6 B cells in a single experiment (DeKosky et al., 2015) (Fig. 8C). Similarly, natively paired single-chain variable fragments (scFvs) can be generated in droplets. Subsequently, these scFvs can be expressed in form of yeast display libraries and screened for antigen-binding prior to sequencing (Adler et al., 2017a, 2017b).

Similar to the sequencing of BCR repertoires, corresponding methods for the characterization of T-cell receptor (TCR) repertoires have been developed, given the structural similarity and immunological function: TCR is a member of the immunoglobulin superfamily, found on the surface of T cells. It recognizes the complex of processed antigens and major histocompatibility complex (MHC). In humans, 95% of T cells express heterogeneous TCRs composed of an alpha (α) chain and a beta (β) chain whereas the other 5% of T cells express gamma (γ) and delta (δ) chains. Knowledge on the TCR repertoire and pairing is not only relevant for basic immunology, but as well for many clinical applications. For example, the treatment of cancer, viral infections and bacterial diseases with T cell-based therapies has seen great advances over the past decades (Restifo et al., 2012; Lam and Bollard, 2013; Parida et al., 2015). Two kinds of T cell immunotherapies are widely used: One is the infusion of autologous antigen-reactive T cells expanded *in vitro*, while the other is the infusion of *de novo*-generated antigen-reactive T cell populations produced by introducing genes encoding antigen-reactive TCRs. For both approaches, identifying paired TCR α-chains and TCR β-chains sequences of antigen-reactive TCRs at the single-cell level is of substantial interest. However, conventional TCR library preparation methods in combination with high-throughput sequencing only provide unpaired TCR-α or TCR-β gene sequences that only reveal 'half the truth' (Mamedov et al., 2011; Kitaura et al., 2016).

To improve the throughput for single-cell TCR sequencing, a non-microfluidic emulsion-based RT-PCR approach was developed (generating emulsions using a stirrer (Williams et al., 2006);), which allows encapsulation, lysis of single T cells, reverse-transcription of mRNA and overlapping PCR of TCR-α and β-chain variable regions of single T cells in droplets (Turchaninova et al., 2013). A new strategy using PCR suppression was also introduced to decrease the noise detected in downstream high-throughput paired-end Illumina sequencing. Briefly, the authors added an excessive amount of oligonucleotides that are complementary to the 3′-end of free, non-overlapping alpha and beta chain PCR products, with an additional seven nonsense nucleotides extension. This way, non-fused alpha or beta chains cannot fuse with those from other droplets after breaking the emulsion. In one million PBMCs, more than 700 α-ß-pairs were unambiguously identified. To determine the detection sensitivity, 1000 T cell clones (C1A) were added as a spike-in to one million PBMCs, and from two of three repeats, internal control clone C1A was detected, which indicated that the detection resolution was about 1000 clonal T cells per million PBMCs (approximately 0.2% of all T cells) (Turchaninova et al., 2013). The Georgiou lab performed analogous studies using microfluidic drop makers, exploiting workflows similar to those for the sequencing of B-cell repertoires (Fig. 8C). This resulted in detailed protocols for the screening of millions of lymphocytes at an efficiency of >97%, within just 12 h (McDaniel et al., 2016).

In addition to just sequencing the TCR chains, one can also perform global single-cell transcriptomics to get more detailed
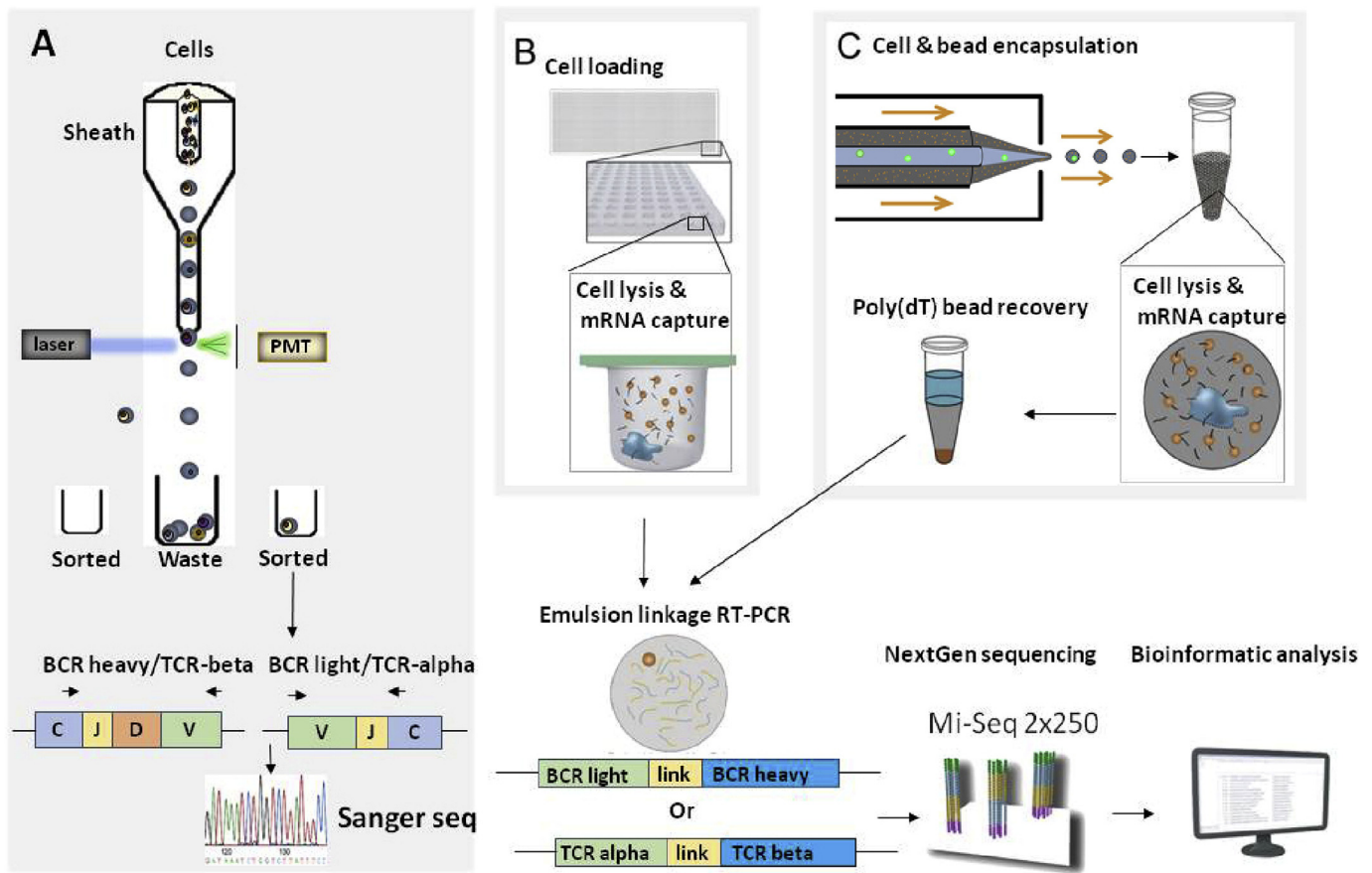
Fig. 8. Approaches for BCR and TCR repertoire sequencing. (A) Schematic workflow of FACS-based single cell sorting and subsequent PCR for the amplification and sequencing of paired BCR-heavy and BCR-light chains or TCR-alpha and TCR-beta. (B) Schematic workflow of nanowell-based BCR and TCR repertoire sequencing. Single cells and poly(dT) microbeads are deposited into nanowells. Cells are lyzed (blue) and the released mRNA (black) anneals to the poly(dT) beads (orange). The beads are then recovered and emulsified for cDNA synthesis and linkage PCR to generate $V_H:V_L$ cDNA products of approximately 850−base pairs. Overlapped TCR-α and TCR-β V-regions can be generated in a similar way. Next-generation sequencing is performed to sequence the linked strands. Adapted by permission from Macmillan Publishers Ltd: Nature Biotechnology (DeKosky et al., 2013), copyright (2015). (C) Schematic workflow of droplet-based ultra-high throughput BCR or TCR sequencing from single B cells or T cells. Instead of using nanowells, an asymmetric flow-focusing nozzle is used to co-encapsulate single cells (blue, highlighted by green circles) and poly(dT) magnetic beads (gray, highlighted by orange circles) together with lysis buffer. In individual droplets, cells are lyzed and mRNAs are annealed to poly(dT) beads which are subsequently recovered and emulsified for cDNA synthesis and linkage PCR to generate $V_H:V_L$ cDNA products of approximately 850−base pairs. Overlapped Vα:Vβ cDNA can be generated in a similar way. Next-generation sequencing is performed to sequence the linked strands. Adapted by permission from Macmillan Publishers Ltd: Nature Medicine (DeKosky et al., 2015), copyright (2013). (For interpretation of the references to colour in this figure legend, the reader is referred to the web version of this article.)

information on T-cell biology. Sarah Teichmann's lab developed the TraCeR package, a tool that connects the T cell specificity, represented by TCR, with its functional response, represented by its transcriptome, at a single-cell level. It can analyze data obtained from the valve-based Fluidigm C1 system or, in theory, any other single-cell transcriptomics platform. TraCeR revealed novel or poorly characterized phenotypic subtypes in conjunction with the analysis of their TCR sequences, where in a mouse *Salmonella* infection model, members of expanded T cell clonotype span early activated CD4^{+} T cells, as well as mature effector and memory cells (Stubbington et al., 2016). Whole transcriptome studies of individual murine CD4^{+} memory cells furthermore showed that the response to stimulation shows significantly higher transcriptional variation with increasing age of the donors (Martinez-Jimenez et al., 2017). Together with the previously known decrease of the B- and T-cell repertoires in elderly subjects (Dunn-Walters, 2016; Goronzy et al., 2015) this could be a hallmark feature of aging.

The power of single T-cell RNA-seq studies can probably be increased further using droplet-based single-cell RNA-seq methods such as DropSeq or InDrop (Tang et al., 2009; Klein et al., 2015). In these approaches, beads displaying uniquely barcoded polyT

primers (all polyT primers on the same bead show the same barcode, but the barcodes differ between different beads) are co-encapsulated into droplets together with single-cells. Upon cell lysis inside the droplets, all cellular mRNAs hybridize with the polyT primers and thus get barcoded during a subsequent RT-PCR step. After sequencing, all cDNAs showing the same barcode (corresponding to mRNAs coming from the same cell) are clustered revealing the global transcriptome of individual cells. Alternatively to using droplets as microcompartments such studies can also be carried out in nanowell-based systems, enabling similar throughputs for single-cell transcriptomics (Bose et al., 2015; Gierahn et al., 2017; Yuan and Sims, 2016). Taken together, microfluidic technology allows massively parallelized sequencing of single T-cells, not only to achieve correct pairing and comprehensive analysis of the immune repertoire, but also for a deeper understanding of fundamental biological processes.

6. Outlook

Microfluidic systems have significantly advanced our understanding of immunology over the past decade. They provide

solutions for many different applications and allow studies which were previously unthinkable. This is also a unique opportunity for new therapeutic approaches: For example, a better understanding of immune signaling and immune cell migration is of major interest for cancer therapy. The possibility of studying T-cell activation at the single-cell level, or even to pair individual immune and cancer cells should have tremendous impact on the understanding of cancer immunosurveillance, a theme which has recently attracted particular attention in the context of immune-checkpoint molecules (Khandelwal et al., 2015). Furthermore, microfluidics will ultimately allow the screening of B cells from humans (e.g. disease survivors, cancer patients) to derive highly specific therapeutic antibodies which, based on their human origin, should be free of any undesired side effects. Moreover, microfluidic antibody screens can also be "reversed" to identify promising vaccine candidates starting with neutralizing antibodies: We have recently established a corresponding single-virus droplet-based microfluidics platform for analyzing the binding of neutralizing antibodies to millions of HIV-1 particles (Chaipan et al., 2017). Efficient binding indicates stable and accessible display of neutralizing epitopes and hence promising vaccine candidates. Lastly, the systematic sequencing of immune repertoires will give further insights into aging and autoimmune diseases. In short, microfluidic approaches will contribute significantly to future biomedical discoveries.

On the technology side, we can also expect further breakthroughs: Just recently, a method for combined transcriptome and protein analysis of single-cells has been described (Stoeckius et al., 2017). Furthermore, there is continuous progress in increasing the throughput, robustness and multiplexing capabilities of microfluidic systems (Shembekar et al., 2016; Xi et al., 2017; Frenzel and Merten, 2017). Ultimately this will allow ever more complex studies, and we are curious to see spectacular results in the coming years.

Acknowledgements

References

Adler, A.S., et al., 2017a. Rare, high-affinity mouse anti-PD-1 antibodies that function in checkpoint blockade, discovered using microfluidics and molecular genomics. MAbs 0.

Adler, A.S., et al., 2017b. Rare, high-affinity anti-pathogen antibodies from human repertoires, discovered using microfluidics and molecular genomics. MAbs 0.

Ambravaneswaran, V., et al., 2010. Directional decisions during neutrophil chemotaxis inside bifurcating channels. Integr. Biol. Quant. Biosci. Nano Macro 2 (11–12), 639–647.

Beltman, J.B., Marée, A.F.M., de Boer, R.J., 2009. Analysing immune cell migration. Nat. Rev. Immunol. 9 (11), 789–798.

Bose, S., et al., 2015. Scalable microfluidics for single-cell RNA printing and sequencing. Genome Biol. 16, 120.

Brownlie, R.J., Zamoyska, R., 2013. T cell receptor signalling networks: branched, diversified and bounded. Nat. Rev. Immunol. 13 (4), 257–269.

Busse, C.E., et al., 2014. Single-cell based high-throughput sequencing of full-length immunoglobulin heavy and light chain genes. Eur. J. Immunol. 44 (2), 597–603.

Carter, P., 2001. Improving the efficacy of antibody-based cancer therapies. Nat. Rev. Cancer 1 (2), 118–129.

Casadevall, A., Dadachova, E., Pirofski, L.A., 2004. Passive antibody therapy for infectious diseases. Nat. Rev. Microbiol. 2 (9), 695–703.

Chaipan, C., et al., 2017. Single-virus droplet microfluidics for high-throughput screening of neutralizing epitopes on HIV particles. Cell Chem. Biol. 24 (6), 751–757.

Chan, A.C., Carter, P.J., 2010. Therapeutic antibodies for autoimmunity and inflammation. Nat. Rev. Immunol. 10 (5), 301–316.

Chan, C.J., Smyth, M.J., Martinet, L., 2014. Molecular mechanisms of natural killer cell activation in response to cellular stress. Cell Death Differ. 21 (1), 5–14.

Chen, L.P., Flies, D.B., 2013. Molecular mechanisms of T cell co-stimulation and co-inhibition (vol. 13, pg 27, 2013). Nat. Rev. Immunol. 13 (7).

Choi, K., et al., 2012. Digital microfluidics. Annu. Rev. Anal. Chem. 5, 413–440, 5.

Chokkalingam, V., et al., 2013. Probing cellular heterogeneity in cytokine-secreting immune cells using droplet-based microfluidics. Lab Chip 13 (24), 4740–4744.

Chu, V.T., et al., 2011. Eosinophils are required for the maintenance of plasma cells in the bone marrow. Nat. Immunol. 12 (2), 151–159.

Crough, T., Khanna, R., 2009. Immunobiology of human cytomegalovirus: from bench to bedside. Clin. Microbiol. Rev. 22 (1), 76–98.

DeKosky, B.J., et al., 2013. High-throughput sequencing of the paired human immunoglobulin heavy and light chain repertoire. Nat. Biotechnol. 31 (2), 166–169.

DeKosky, B.J., et al., 2015. In-depth determination and analysis of the human paired heavy- and light-chain antibody repertoire. Nat. Med. 21 (1), 86–91.

Doria-Rose, N.A., et al., 2014. Developmental pathway for potent V1V2-directed HIV-neutralizing antibodies. Nature 509 (7498), 55–62.

Dunn-Walters, D.K., 2016. The ageing human B cell repertoire: a failure of selection? Clin. Exp. Immunol. 183 (1), 50–56.

Dura, B., et al., 2015. Profiling lymphocyte interactions at the single-cell level by microfluidic cell pairing. Nat. Commun. 6, 5940.

Dura, B., et al., 2016. Longitudinal multiparameter assay of lymphocyte interactions from onset by microfluidic cell pairing and culture. Proc. Natl. Acad. Sci. U. S. A. 113 (26), E3599–E3608.

Ecker, D.M., Jones, S.D., Levine, H.L., 2015. The therapeutic monoclonal antibody market. Mabs 7 (1), 9–14.

Eicher, D., Merten, C.A., 2011. Microfluidic devices for diagnostic applications. Expert Rev. Mol. Diagn 11 (5), 505–519.

El Debs, B., et al., 2012. Functional single-cell hybridoma screening using droplet-based microfluidics. Proc. Natl. Acad. Sci. U. S. A. 109 (29), 11570–11575.

Frenzel, D., Merten, C.A., 2017. Microfluidic train station: highly robust and multiplexable sorting of droplets on electric rails. Lab Chip 17, 1024–1030.

Georgiou, G., et al., 2014. The promise and challenge of high-throughput sequencing of the antibody repertoire. Nat. Biotechnol. 32 (2), 158–168.

Gierahn, T.M., et al., 2017. Seq-Well: portable, low-cost RNA sequencing of single cells at high throughput. Nat. Methods 14 (4), 395-+.

Goronzy, J.J., et al., 2015. High-throughput sequencing insights into T-cell receptor repertoire diversity in aging. Genome Med. 7.

Haessler, U., et al., 2011. Dendritic cell chemotaxis in 3D under defined chemokine gradients reveals differential response to ligands CCL21 and CCL19. Proc. Natl. Acad. Sci. U. S. A. 108 (14), 5614–5619.

Han, Q., et al., 2012. Polyfunctional responses by human T cells result from sequential release of cytokines. Proc. Natl. Acad. Sci. 109 (5), 1607–1612.

Hendershot, L.M.S.,R., 2003. In: Honjo, T., Alt, F., Neuberger, M. (Eds.), Molecular Biology of B Cells.

Hoogenboom, H.R., 2005. Selecting and screening recombinant antibody libraries. Nat. Biotechnol. 23 (9), 1105–1116.

Huang, C.P., et al., 2009. Engineering microscale cellular niches for three-dimensional multicellular co-cultures. Lab Chip 9 (12), 1740–1748.

Hummer, D., et al., 2016. Single cells in confined volumes: microchambers and microdroplets. Lab Chip 16 (3), 447–458.

Jain, N.G., et al., 2015. Microfluidic mazes to characterize T-cell exploration patterns following activation in vitro. Integr. Biol. Quant. Biosci. Nano Macro 7 (11), 1423–1431.

Jin, A., et al., 2009. A rapid and efficient single-cell manipulation method for screening antigen-specific antibody-secreting cells from human peripheral blood. Nat. Med. 15 (9), 1088–1092.

Junkin, M., et al., 2016. High-content quantification of single-cell immune dynamics. Cell Rep. 15 (2), 411–422.

Kaiko, G.E., et al., 2008. Immunological decision-making: how does the immune system decide to mount a helper T-cell response? Immunology 123 (3), 326–338.

Khandelwal, N., et al., 2015. A high-throughput RNAi screen for detection of immune-checkpoint molecules that mediate tumor resistance to cytotoxic T lymphocytes. EMBO Mol. Med. 7 (4), 450–463.

Kitaura, K., et al., 2016. A new high-throughput sequencing method for determining diversity and similarity of T cell receptor (TCR) alpha and beta repertoires and identifying potential new invariant TCR alpha chains. BMC Immunol. 17 (1), 38.

Klein, A.M., et al., 2015. Droplet barcoding for single-cell transcriptomics applied to embryonic stem cells. Cell 161 (5), 1187–1201.

Kohler, G., Milstein, C., 1975. Continuous cultures of fused cells secreting antibody of predefined specificity. Nature 256 (5517), 495–497.

Konry, T., et al., 2011. Droplet-based microfluidic platforms for single T cell secretion analysis of IL-10 cytokine. Biosens. Bioelectron. 26 (5), 2707–2710.

Kotsovilis, S., Andreakos, E., 2014. Therapeutic human monoclonal antibodies in inflammatory diseases. Methods Mol. Biol. 1060, 37–59.

Krebber, A., et al., 1997. Reliable cloning of functional antibody variable domains from hybridomas and spleen cell repertoires employing a reengineered phage display system. J. Immunol. Methods 201 (1), 35–55.

Krummel, M.F., Bartumeus, F., Gérard, A., 2016. T cell migration, search strategies and mechanisms. Nat. Rev. Immunol. 16 (3), 193–201.

Kwakkenbos, M.J., et al., 2010. Generation of stable monoclonal antibody-producing B cell receptor-positive human memory B cells by genetic programming. Nat. Med. 16 (1), 123–U164.

Lam, S., Bollard, C., 2013. T-cell therapies for HIV. Immunotherapy 5 (4), 407–414.

Lee, K.H., et al., 2002. T cell receptor signaling precedes immunological synapse formation. Science 295 (5559), 1539–1542.

Lin, F., Butcher, E.C., 2006. T cell chemotaxis in a simple microfluidic device. Lab Chip 6 (11), 1462–1469.

Little, M., et al., 2000. Of mice and men: hybridoma and recombinant antibodies. Immunol. Today 21 (8), 364—370.

Liu, X.S., Mardis, E.R., 2017. Applications of immunogenomics to cancer. Cell 168 (4), 600—612.

Love, J.C., et al., 2006. A microengraving method for rapid selection of single cells producing antigen-specific antibodies. Nat. Biotechnol. 24 (6), 703—707.

Lu, Y., et al., 2015. Highly multiplexed profiling of single-cell effector functions reveals deep functional heterogeneity in response to pathogenic ligands. Proc. Natl. Acad. Sci. U. S. A. 112 (7), E607—E615.

Ma, C., et al., 2011. A clinical microchip for evaluation of single immune cells reveals high functional heterogeneity in phenotypically similar T cells. Nat. Med. 17 (6), 738—743.

Macosko, E.Z., et al., 2015. Highly parallel genome-wide expression profiling of individual cells using nanoliter droplets. Cell 161 (5), 1202—1214.

Mahata, B., et al., 2014. Single-cell RNA sequencing reveals T helper cells synthesizing steroids de novo to contribute to immune homeostasis. Cell Rep. 7 (4), 1130—1142.

Malissen, B., et al., 2014. Integrative biology of T cell activation. Nat. Immunol. 15 (9), 790—797.

Mamedov, I.Z., et al., 2011. Quantitative tracking of T cell clones after haematopoietic stem cell transplantation. EMBO Mol. Med. 3 (4), 201—207.

Martinez-Jimenez, C.P., et al., 2017. Aging increases cell-to-cell transcriptional variability upon immune stimulation. Science 355 (6332), 1433-+.

Mazutis, L., et al., 2013. Single-cell analysis and sorting using droplet-based microfluidics. Nat. Protoc. 8 (5), 870—891.

McDaniel, J.R., et al., 2016. Ultra-high-throughput sequencing of the immune receptor repertoire from millions of lymphocytes. Nat. Protoc. 11 (3), 429—442.

Michel, J.J., Griffin, P., Vallejo, A.N., 2016. Functionally diverse NK-like T cells are effectors and predictors of successful aging. Front. Immunol. 7.

Miraglia, S., et al., 1999. Homogeneous cell- and bead-based assays for high throughput screening using fluorometric microvolume assay technology. J. Biomol. Screen 4 (4), 193—204.

Mosser, D.M., Edwards, J.P., 2008. Exploring the full spectrum of macrophage activation. Nat. Rev. Immunol. 8 (12), 958—969.

Nandagopal, S., Wu, D., Lin, F., 2011. Combinatorial guidance by CCR7 ligands for T lymphocytes migration in co-existing chemokine fields. PLoS One 6 (3), e18183.

Nelson, A.L., Dhimolea, E., Reichert, J.M., 2010. Development trends for human monoclonal antibody therapeutics. Nat. Rev. Drug Discov. 9 (10), 767—774.

Ogunniyi, A.O., et al., 2009. Screening individual hybridomas by microengraving to discover monoclonal antibodies. Nat. Protoc. 4 (5), 767—782.

Pabst, O., Hazanov, H., Mehr, R., 2015. Old questions, new tools: does next-generation sequencing hold the key to unraveling intestinal B-cell responses? Mucosal Immunol. 8 (1), 29—37.

Parida, S.K., et al., 2015. T-cell therapy: options for infectious diseases. Clin. Infect. Dis. 61 (Suppl. 3), S217—S224.

Peine, M., et al., 2013. Stable t-bet+GATA-3+ Th1/Th2 hybrid cells arise in vivo, can develop directly from naive precursors, and limit immunopathologic inflammation. PLOS Biol. 11 (8), e1001633.

Phetsouphanh, C., Zaunders, J.J., Kelleher, A.D., 2015. Detecting antigen-specific T cell responses: from bulk populations to single cells. Int. J. Mol. Sci. 16 (8), 18878—18893.

Preira, P., et al., 2016. The leukocyte-stiffening property of plasma in early acute respiratory distress syndrome (ARDS) revealed by a microfluidic single-cell study: the role of cytokines and protection with antibodies. Crit. CareLond.n, Engl. 20, 8.

Qiu, X., et al., 2014. Reversion of advanced Ebola virus disease in nonhuman primates with ZMapp. Nature 514 (7520), 47—53.

Reddy, S.T., et al., 2010. Monoclonal antibodies isolated without screening by analyzing the variable-gene repertoire of plasma cells. Nat. Biotechnol. 28 (9), 965—969.

Restifo, N.P., Dudley, M.E., Rosenberg, S.A., 2012. Adoptive immunotherapy for cancer: harnessing the T cell response. Nat. Rev. Immunol. 12 (4), 269—281.

Ricart, B.G., et al., 2011. Dendritic cells distinguish individual chemokine signals through CCR7 and CXCR4. J. Immunol. 186 (1), 53—61 (Baltimore, Md.: 1950).

Ricart, B.G., et al., 2011. Measuring traction forces of motile dendritic cells on micropost arrays. Biophys. J. 101 (11), 2620—2628.

Sarkar, S., et al., 2015. T cell dynamic activation and functional analysis in nanoliter droplet microarray. J. Clin. Cell. Immunol. 6 (3).

Sarkar, S., et al., 2016. Dynamic analysis of immune and cancer cell interactions at single cell level in microfluidic droplets. Biomicrofluidics 10 (5), 054115.

Schmidt, T., Sester, M., 2013. Detection of antigen-specific T cells based on intra-cellular cytokine staining using flow-cytometry. In: Bailer, S.M., Lieber, D. (Eds.), Virus-host Interactions. Humana Press, pp. 267—274.

Shalek, A.K., et al., 2013. Single-cell transcriptomics reveals bimodality in expression and splicing in immune cells. Nature 498 (7453), 236—240.

Shembekar, N., et al., 2016. Droplet-based microfluidics in drug discovery, transcriptomics and high-throughput molecular genetics. Lab Chip 16 (8), 1314—1331.

Simon Tickle, R.A., Brown, Derek, Griffiths, Meryn, Lightwood, Daniel, Lawson, Alastair, 2009. High-throughput screening for high affinity antibodies. J. Assoc. Lab. Autom. 14 (5), 303—307.

Singhal, A., Haynes, C.A., Hansen, C.L., 2010. Microfluidic measurement of antibody-antigen binding kinetics from low-abundance samples and single cells. Anal. Chem. 82 (20), 8671—8679.

Skirgello, O.E., et al., 2006. Inhibitory antibodies to human angiotensin-converting enzyme: fine epitope mapping and mechanism of action. Biochemistry 45 (15), 4831—4847.

Sliwkowski, M.X., Mellman, I., 2013. Antibody therapeutics in cancer. Science 341 (6151), 1192—1198.

Stoeckius, M., et al., 2017. Simultaneous epitope and transcriptome measurement in single cells. Nat. Comm. 14, 865—868.

Story, C.M., et al., 2008. Profiling antibody responses by multiparametric analysis of primary B cells. Proc. Natl. Acad. Sci. U. S. A. 105 (46), 17902—17907.

Strait, R.T., et al., 2015. IgG1 protects against renal disease in a mouse model of cryoglobulinaemia. Nature 517 (7535), 501—504.

Stubbington, M.J., et al., 2016. T cell fate and clonality inference from single-cell transcriptomes. Nat. Methods 13 (4), 329—332.

Tang, F., et al., 2009. mRNA-Seq whole-transcriptome analysis of a single cell. Nat. Methods 6 (5), 377—382.

Tiller, T., et al., 2008. Efficient generation of monoclonal antibodies from single human B cells by single cell RT-PCR and expression vector cloning. J. Immunol. Methods 329 (1—2), 112—124.

Tiller, T., Busse, C.E., Wardemann, H., 2009. Cloning and expression of murine Ig genes from single B cells. J. Immunol. Methods 350 (1—2), 183—193.

Traggiai, E., et al., 2004. An efficient method to make human monoclonal antibodies from memory B cells: potent neutralization of SARS coronavirus. Nat. Med. 10 (8), 871—875.

Tscharke, D.C., et al., 2015. Sizing up the key determinants of the CD8(+) T cell response. Nat. Rev. Immunol. 15 (11), 705—716.

Turchaninova, M.A., et al., 2013. Pairing of T-cell receptor chains via emulsion PCR. Eur. J. Immunol. 43 (9), 2507—2515.

Upert, G., Merten, C.A., Wennemers, H., 2010. Nanoliter plates—versatile tools for the screening of split-and-mix libraries on-bead and off-bead. Chem. Commun. Camb 46 (13), 2209—2211.

Vyawahare, S., Griffiths, A.D., Merten, C.A., 2010. Miniaturization and parallelization of biological and chemical assays in microfluidic devices. Chem. Biol. 17 (10), 1052—1065.

Weinstein, J.A., et al., 2009. High-throughput sequencing of the zebrafish antibody repertoire. Science 324 (5928), 807—810.

Williams, R., et al., 2006. Amplification of complex gene libraries by emulsion PCR. Nat. Methods 3 (7), 545—550.

Wrammert, J., et al., 2008. Rapid cloning of high-affinity human monoclonal antibodies against influenza virus. Nature 453 (7195), 667—671.

Wu, X., et al., 2010. Rational design of envelope identifies broadly neutralizing human monoclonal antibodies to HIV-1. Science 329 (5993), 856—861.

Wu, X., et al., 2011. Focused evolution of HIV-1 neutralizing antibodies revealed by structures and deep sequencing. Science 333 (6049), 1593—1602.

Xi, H.-D., et al., 2017. Active droplet sorting in microfluidics: a review. Lab Chip 17, 751—771.

Yaari, G., Kleinstein, S.H., 2015. Practical guidelines for B-cell receptor repertoire sequencing analysis. Genome Med. 7, 121.

Yuan, J., Sims, P.A., 2016. An automated microwell platform for large-scale single cell RNA-seq. Sci. Rep. 6, 33883.